ABSTRACT

BROWNFIELD, ANDREW MAHONEY. A Study of Hyaluronidases and UDP-Glucose Dehydrogenase as Contributing Factors to Prostate Cancer Progression. (Under the direction of Dr. Melanie Simpson).

In 2020, prostate cancer was the most frequently diagnosed cancer in American men and it is estimated that 1 in 9 men will receive this diagnosis in their lifetime. Two essential enzymes that impact prostate cancer progression are UDP-glucose dehydrogenase (UGDH) and hyaluronidase (Hyal). Hyaluronic acid (HA) is an essential component of the extracellular matrix and is critical to many cellular functions including cell adhesion, cell proliferation, infection response, and cell signaling. In tissues, HA is involved in angiogenesis, morphogenesis, protection, cushioning, and lubrication. Dysregulated HA metabolism is a hallmark of cancer progression, metastasis, as well as chronic inflammatory diseases. HA is synthesized by hyaluronan synthases and enzymatically cleaved by hyaluronidases into smaller fragments. There are five human Hyals (hHyal): Hyal1-4 and PH-20 (expressed only in sperm); each with a distinct set of characteristics. Despite the well-known importance of proper HA regulation, there remains much uncertainty in the literature about the expression, characteristics, catalytic ability, and substrate preference of each of the Hyals. Here, a methodology is presented for the expression, purification, and catalytic characterization of Hyals 1-4. This research adds to the body of knowledge regarding the Hyal family of proteins and serves as an easy reference for the creation of Hyal proteins so they can be enzymatically studied in greater detail.

UGDH is a toroidal homohexamer that catalyzes the two step NAD+-dependent conversion of UDP-glucose to UDP-glucuronate. UGDH is the sole creator of UDP-glucuronate, which is a key component in three cellular functions: HA production, glycosaminoglycan (such as chondroitin sulfate) synthesis, and glucuronidation of hormones via UDP-

glucuronosyltransferases. UGDH is highly expressed in the prostate and the overexpression of human UGDH (hUGDH) has been noted in several cancers. Knocking down or inhibiting hUGDH results in decreased tumor cell motility and tumor growth. Therefore, development of a small molecule capable of limiting the catalytic ability of overexpressed hUGDH represents an opportunity to combat prostate cancer progression. To that end, our lab screened for hUGDH inhibitory peptides and validated the top hits using synthetic peptides. In this work, X-ray crystallography was used to molecularly determine how the most promising peptide (P4) impacts UGDH conformation. Using an approximately 3.25 Å dataset collected at SER-CAT, we were able to show that when exposed to P4, hUGDH adopts a global shape and catalytic residue orientations most like an inactive state between the UDP-xylose inhibited and active hUGDH, referred to as E*. Overall, this suggests that P4 can be used as a point of reference for drug development against overexpressed hUGDH.

The work presented here serves as a foundation for further investigations into HA metabolism and hUGDH control, with the goal of combating abnormal hUGDH expression and HA dysregulations. A more comprehensive understanding of these enzymes and the ability to use pharmacological agents to control them, will contribute to alleviating inflammatory disease and tumor progression.

A Study of Hyaluronidases and UDP-Glucose Dehydrogenase as Contributing Factors to Prostate Cancer Progression.

by
Andrew Brownfield

A thesis submitted to the Graduate Faculty of
North Carolina State University
in partial fulfillment of the
requirements for the degree of
Master of Science

Biochemistry

Raleigh, North Carolina
2021

APPROVED BY:

_____	_____
Dr. Melanie Simpson Committee Chair	Dr. Joseph Barycki
_____	
Dr. Arion Kennedy	

DEDICATION

I would like to dedicate this work to my family, my girlfriend, and my friends. I love you all and you are unquestionably the most important parts of my life.

My parents have shaped me into a critical thinker and a hard worker, traits that are the bedrock of my past and future success. Also, they have always believed in me and encouraged me to do my best and chase happiness. My sister has always been there for me, supported me and been a source of laughter and joy.

Particularly during graduate school, I owe an immense amount of appreciation to my girlfriend, Sarah Zwicker. Graduate school is hard; the support, love, and laughter she continually gave me was invaluable. My time in Raleigh and graduate school would have been unimaginably difficult without her.

Finally, I am deeply grateful to my friends for always being there for me and being endless sources of joy. I am extremely lucky to have the many and variety of friends that I do, and they are a huge part of what makes me happy and successful.

BIOGRAPHY

I was born in Madison, WI to a geriatric physician and a professor of veterinary medicine and grew up in Oregon, WI. My parents fostered an environment of critical thinking and hard work. In every grade, I gravitated towards sciences; learning about the interconnected forces that govern the universe, animal behavior, and human physiology was continually fascinating. I took a broad range of scientific courses and attended the University of Wisconsin - La Crosse to obtain my undergraduate degrees in Biochemistry and Cellular and Molecular Biology. Here, I honed my critical thinking skills and took on an introductory role in undergraduate research.

After college, I worked first as an Analytical Chemist at Covance, where I analyzed submitted samples for vitamin concentrations. I then accepted a position as a Microbiologist at the Wisconsin Veterinary Diagnostic Laboratory, detecting and quantifying viral titers in animal samples. Additionally, I worked on an applied research project to improve a problematic assay, thereby increasing efficiency, sensitivity and decreasing costs. These experiences were key in my preparation and success as a graduate student.

ACKNOWLEDGMENTS

Most importantly, I want to thank Dr. Melanie Simpson and Dr. Joseph Barycki for accepting me into the Biochemistry program and for the continual support and guidance I have received while growing in the lab. With deep gratitude, I have become a more well-rounded, experienced, and successful scientist. Beyond the lab, conversations with either or both of you have been filled with honesty, kindness, and good humor; I will always appreciate that. Additionally, I want to thank and acknowledge Dr. Arion Kennedy for being a supportive faculty member that I was always able to speak candidly with. Also, thank you for a productive rotation period, which helped me settle into life in Raleigh and the program at North Carolina State University.

I also extend sincere thanks to my lab members: Emily Allego, Accola Hudson, Monica Milici and particularly Dr. Brenna Zimmer and Lily Ma. You have all been wonderful lab members and made the often-arduous scientific process much more enjoyable, along with helping me through various experiments by advising or lending a helping hand. Dr. Zimmer, thank you so much for helping me learn novel tasks and being an endless source of information regarding lab procedures, scientific information, and friendship. I am unquestionably a better scientist because of our informative and fruitful scientific discussions. Lily, thank you enormously for selflessly supplying the lab and keeping everything running smoothly, and particularly for all the assistance in my early months in the lab. You helped me get settled and were instrumental in getting my project started that it sometimes felt like you were the brains behind my project, and I was the hands. In short, you were an excellent scientific guide when I really needed one, thank you so much.

Finally, I would like to acknowledge the work and assistance provided by Paul Swartz and Peter Thompson, for helping me utilize complex instruments to glean scientific insights. I was happy to learn from each of you and I enjoyed talking with you about science, but especially enjoyed our deeper conversations about life, graduate school, and anything else. I deeply appreciate that you were both available to troubleshoot, answer questions or provide ideas. Peter, you helped me a lot with NMR and SPR, and Paul, my greatest gratitude for guiding me through X-ray crystallography; it was an extremely complicated process, and I could not have done that project without your help. Thank you so much to both of you.

TABLE OF CONTENTS

LIST OF TABLES

LIST OF FIGURES

CHAPTER 1. INTRODUCTION

Prostate Cancer

According to the American Cancer Society, prostate cancer was the most frequently diagnosed cancer amongst American men in 2020, accounting for an estimated 21% of cancer diagnoses in men and 10% of deaths (1). In 2020, it is estimated that 191,930 men were diagnosed with prostate cancer, with 33,330 deaths due to the disease (1). Ultimately, an estimated 1 in 9 men will be diagnosed with prostate cancer in their lifetime (1), and 1 in 41 men will succumb to prostate cancer (2). The average age of prostate cancer diagnosis is 66 (2), while the median age of death is 80 (3).

Early and thorough screening for prostate cancer remains controversial, with high costs and inconclusive results. Prostate-specific antigen-based (PSA) screening potentially reduces mortality risk but is accompanied with false-positives and biopsy complications (4). Additionally, advanced screening can result in early treatments that may have adverse effects on sexual and urinary health (4). Conversely, prostate cancer mortality rates are generally higher in countries that conduct little or no screening, suggesting that the discovery of early, localized cancer and prompt treatment may compensate for the overdiagnosis and drawbacks associated with PSA-based screening (5, 6). Many men live with prostate cancer and never experience symptoms, and thus would never know that they have the disease without screening. Because of this, the US Preventative Services Task Force recommends that men aged 55 to 69 discuss the PSA-based screen with their clinician to weigh the benefits, costs, and effectiveness of the PSA-based screen (3). Prostate cancer diagnosis rates have been increasing around the world and parallel the increased usage of the PSA-based screen; this has led to more men being diagnosed with localized cancer and at an earlier age (5, 7, 8). Diagnosis rates have also increased in

countries that do not employ the PSA-based screen, suggesting a shift in environmental and lifestyle factors that influence prostate cancer incidence (5, 9). Because prostate cancer is frequently diagnosed early and generally progresses very slowly, early treatment remains controversial, with studies contradicting one another as to whether aggressive treatment on a localized tumor is beneficial (10, 11). Adding to this, most men diagnosed experience a slow-growing or indolent form, while a minority of cases are aggressive (5). Prostate cancer is clearly a clinically heterogeneous disease with an unpredictable trajectory, which makes screening and treatment decisions difficult to make. These challenges and the prevalence of prostate cancer demonstrate the need for a new way of thinking about detecting, understanding, and managing prostate cancer; new prostate cancer interventions are needed to combat this common, costly, and deadly disease.

Molecular analysis of 333 primary prostate carcinomas was able to place 74% of the tumors into seven subtypes according to gene fusions or mutations, with a wide variety in androgen receptor activity (12). Androgen and androgen derivatives are responsible for proper prostate gland formation and are needed in prostate cancer pathogenesis and progression (13). Inoperable tumors present at diagnosis are treated by androgen deprivation therapy (14). Despite promising initial responses, many tumors aggressively return and continue to grow and metastasize regardless of low androgen level (15, 16). Termed castration resistant prostate cancer (CRPC), these tumors cannot currently be treated and the focus shifts to palliative care (14–16). The mechanisms responsible for the transformation to a castration resistant state are convoluted, unknown, and are the focus of much research. However, it is known that androgens are managed in the glucuronidation pathway, and that the enzyme UDP-glucose dehydrogenase (UGDH) is responsible for the creation of glucuronidation precursors. Human UGDH (hUGDH) is highly

expressed in the prostate (17), upregulated in prostate cancer (18), and is a critical regulating enzyme that can alter the progression of prostate cancer (19). In addition to UGDH, hyaluronic acid (HA) metabolism has been shown to influence prostate cancer progression and metastasis (20–25). UGDH and hyaluronidase (Hyal) are crucial enzymes that maintain proper cell function and are thus of great interest to researchers who are aiming to improve therapy options for those struggling with dysregulated UDP-glucose or hyaluronic acid metabolism.

Structure, function, and importance of UDP-glucose dehydrogenase

UGDH is an essential cytosolic enzyme that uses NAD^+ in the oxidation of UDP-glucose (UDP-glc) to UDP-glucuronate (UDP-glcA), a precursor with three downstream fates. UDP-glcA is a required substrate in the production of HA at the plasma membrane, utilized by UDP-glucuronosyltransferase (UGT) enzymes in the endoplasmic reticulum for dihydrotestosterone (DHT) elimination, and converted into UDP-xylose for proteoglycan (PG) synthesis at the Golgi (Fig. 1) (26, 27). Structurally, eukaryotic UGDH is a hexamer that is constructed by three homodimers forming a donut-shaped quaternary structure (28). The purified apoenzyme equilibrates between its dimeric, tetrameric and hexameric states, with the latter assembly having optimal enzymatic activity (29, 30). Mutagenesis, kinetic and biophysical studies have shown that the human UGDH (hUGDH) hexamer exists in three conditions: an active (E), inactive (E*) or UDP-xylose inhibited (E^{Ω}) hexamer (30–39). A dynamic hexameric hUGDH conformation is critical to optimal enzyme function, which was demonstrated by the mutagenesis of key residues K94 (34) or T325 (29), and resulted in dimeric-only enzymes with reduced activity. The importance of a dynamic enzyme was shown using photoactivated cross-linking (40) or by deleting V132 (35), both of which resulted in the creation of obligate hexamers with decreased

activity. Furthermore, mutations that disrupt the quaternary structure were shown to reduce the stability of UGDH expression and result in a variety of health impairments (41–43).

The first crystal structures of UGDH from *Streptococcus pyogenes* and *Caenorhabditis elegans* (28) were used to determine the two-step oxidation catalytic mechanism. UGDH catalyzes the oxidation of UDP-glc to UDP-glcA using NAD^+, with the N-terminus and C-terminus being responsible for NAD^+ and UDP-glc binding, respectively (44). There are multiple proposed mechanisms, each having supporting evidence (44, 45). In hUGDH, lysine (Lys^{204}), threonine (Thr^{118}), aspartate (Asp^{264}) and asparagine (Asn^{208}) are responsible for UDP-glc stabilization, resulting in a two-electron oxidation of the alcohol to an aldehyde intermediate, simultaneously generating NADH from NAD^+ (46–49). In the second step, a highly conserved

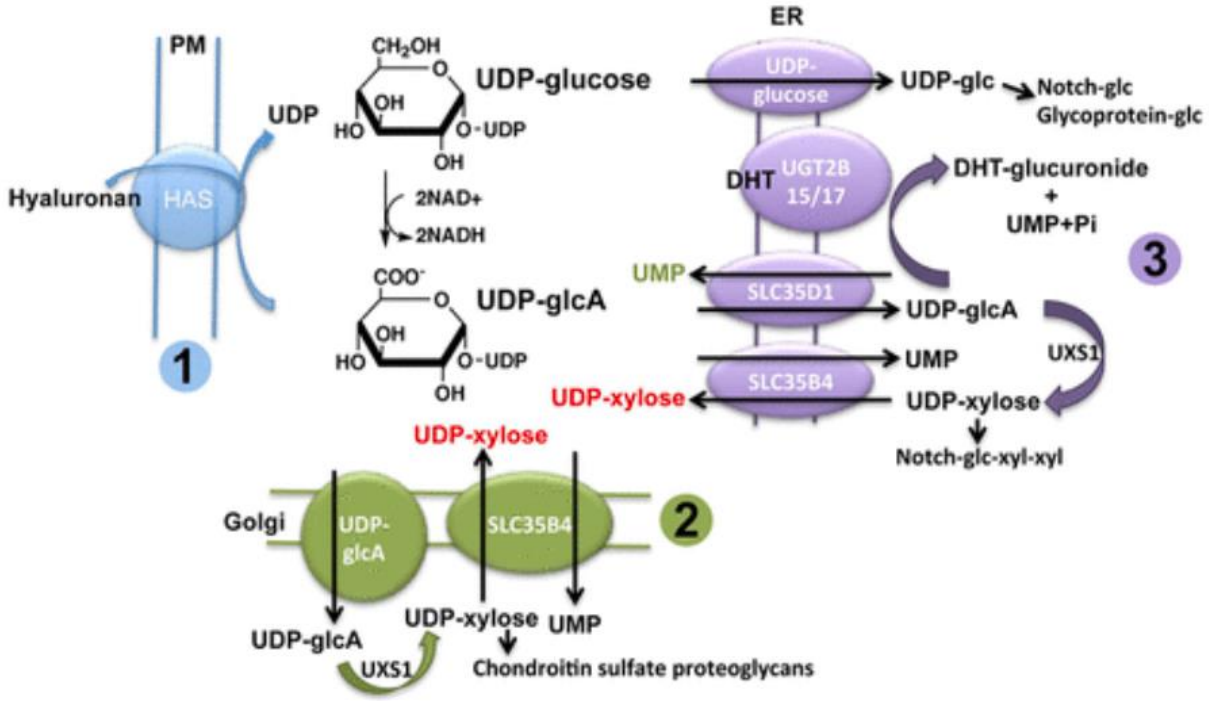

Figure 1 Subcellular distribution of UDP-glucuronate and downstream pathways. UDP-glucose dehydrogenase (UGDH) catalyzes the cytosolic NAD-dependent oxidation of UDP-glucose to UDP-glucuronate (UDP-glcA), which is a critical upstream precursor for three possible processes: (1) hyaluronan synthesis at the plasma membrane; (2) UDP-xylose and proteoglycan synthesis in the Golgi; and (3) hormone (e.g., DHT) glucuronidation in the ER. UDP-glcA is transported into the lumens of ER and Golgi by specific antiporters of the SLC35 class that concurrently export UMP, the leaving group released by UDP-sugar consumption. UDP-glcA is converted to UDP-xylose in the ER and Golgi by UDP-xylose synthase (UXS1). Abbreviations: DHT, dihydrotestosterone; UDP, uridine diphosphate; UMP, uridine monophosphate; PM, plasma membrane. From (27).

cysteine residue (Cys^{260}) acts as an attacking nucleophile to create a thiohemiacetal intermediate, which requires the release of 2 electrons to form another NADH, thereby converting the aldehyde to a carboxylic acid, which creates UDP-glcA (44, 47–49). Importance of the catalytic cysteine residue is supported by the creation of C260A and C260S point mutants, which resulted in elimination or severely decreased catalytic ability of UGDH, respectively (50).

A recently proposed catalytic mechanism postulates that the intermediate aldehyde is bypassed by an NAD^+-dependent nucleophilic substitution (S_N2) reaction, where Cys^{260} and NAD^+ simultaneously attack C-6 and remove an electron pair, respectively, creating the thiohemiacetal intermediate (45, 51). This speculative mechanism may help explain unresolved aspects of the aldehyde intermediate mechanisms but requires additional mechanistic studies. The proposed S_N2 mechanism is more 'advanced' than a two-step mechanism utilizing an aldehyde, since elimination of the intermediate increases catalytic efficiency and removes the need for intermediate trapping and stabilizing agents (45).

Because UGDH is entirely responsible for the creation of the critical precursor UDP-glcA, UGDH has a key role in regulating the formation of PGs and glycosaminoglycans (GAG). Hyaluronic acid (HA) is a prominent GAG present in the extracellular matrix (EM), and its elevation is implicated in the progression of several epithelial cancers (23, 52–55). Conversely, decreased HA production by limiting UDP-glcA results in stunted tumor growth (56, 57). These facts and the unique role of hUGDH makes it a prime candidate for drug development (44), and a potential prostate cancer biomarker (18).

Human UGDH has been implicated in the transformation of prostate cancer to CRPC, as a combined treatment of hUGDH knockdown and androgen deprivation alters the PG and GAG expression profiles and decreases androgen sensitivity (26). The prostate acts in response to

hormone signals; when androgens such as DHT are recognized by prostate tissue, hUGDH expression increases, resulting in increased PG and GAG production, as well as androgen glucuronidation (19, 26). These findings support the notion of hUGDH as a factor in prostate cancer progressing to CRPC.

The regulation and inhibition of hUGDH is an important health objective as a tool against cancer progression. In 2008, it was discovered that the polyphenols gallic acid and quercetin were able to inhibit hUGDH, which reduced proliferation of *in vitro* breast cancer cells (58). Additionally, the compound 4-methylumbelliferone (4MU) has been shown to lower hUGDH expression, which decreases the available pool of UDP-glcA (59), thereby slowing breast cancer invasion and colony formation (60), and increasing apoptosis rates in pancreatic tumor cells (61). Together, these findings illustrate the complexity of UGDH regulation and the need to find novel methods to control hUGDH and potentially direct UDP-glcA to a certain downstream pathway to alter cellular metabolism and correct aberrant cellular behavior. The discovery of a precise compound that could allow for accurate control of this critical enzyme would help a large group of men who suffer from prostate cancer and especially CRPC. To create these compounds, structure-function relationships of UGDH with novel molecules need to be elucidated and characterized.

Structure, function, and relevance of hyaluronidases

HA is a linear, extracellular GAG made up of the repeating disaccharide N-acetyl-D-glucosamine and D-glucuronic acid (62, 63). In healthy humans, a single HA polysaccharide is 1,000 - 7,000 kDa and consists of between 2,500-17,500 disaccharides (64). HA is a key component of the extracellular matrix (ECM) that is ubiquitous but especially abundant in the

skin, brain, umbilical cord, cartilage, and connective tissue (65, 66), where it performs the physical functions of tissue cushioning, hydration, lubrication, wound healing and providing a structural framework for intercellular space (66–69). In addition to its numerous important physical functions, HA also interacts with HA-specific binding proteins to serve as a signal molecule that regulates cellular processes such as adhesion, stress, motility, and proliferation (70, 71). These behaviors are key in many normal and disease-promoting processes including morphogenesis, angiogenesis, embryogenesis, healing, inflammation, and tumorigenesis (72–78).

The physical and functional properties of HA are dependent in part by its molecular weight, which in turn is regulated by the interplay of biosynthesis by hyaluronan synthases (HAS1, HAS2, and HAS3) and degradation by hyaluronidases (Hyals) or reactive oxygen species (ROS) (66, 74, 79–82). While ROS can cleave HA in a non-selective fashion (83–85), most HA is cleaved by the Hyal enzymes hydrolyzing the β-1-4 linkage between HA units in a substrate-assisted mechanism (86–88). An additional substrate for Hyal enzymes is chondroitin sulfate (CS), an important structural component of cartilage (89) that aids in compression resistance (90). Although CS is not studied as thoroughly as HA, CS may be beneficial as a dietary supplement in osteoarthritis (91) by promoting cartilage health and increasing HA synthesis (92).

There are six human HYAL genes that create five protein products (Hyal1-4, and PH-20), although why they each appear to have unique substrate preference and catalytic abilities (93) is a mystery that researchers are trying to reveal. Hyaluronidase activity has also been reported in the enzymes CEMIP (94, 95) and TMEM2 (96), but little is known about these relatively new enzymes, and are not the focus of this work.

Because the concentration and molecular weight of HA are key to its behavior, dysregulation of HA metabolism is associated with inflammatory disease severity and cancer aggressiveness (75, 97). Low molecular weight (LMW) HA directly and indirectly initiates a pro-inflammatory response (98, 99), as well as the innate immune response (100), and can mobilize leukocytes (101). These are healthy cellular responses in normal tissue but in cancer, an abundance of low and medium molecular weight HA in the ECM is associated with cell proliferation, ECM degradation, cell migration, enhanced tumor immunity and capillary formation, whereas HMW HA inhibits cell migration and tumor growth (64, 102).

The correlations between cancer progression and dysregulated HA metabolism are numerous (22, 23, 75, 103–107). Relative to normal tissue, rates of synthesis and fragmentation of HA are increased during inflammation, tissue injury and tumorigenesis (108), ultimately leading to increased concentration of smaller HA fragments, remodeled ECM, and altered cell behavior (73). In cancer specifically, the tumor microenvironment (TME) is remodeled by dysregulated HA metabolism to promote progression and metastasis of cells by increased angiogenesis (109), and diminished tumor immune surveillance (110).

There is a strong correlation between high extracellular LMW HA concentration and poor outcomes in breast (53), ovarian (52), prostate (23, 111), colon (54), lung (112), and gastric cancers (113). Overexpression of HAS was shown to accelerate tumor growth and progression (114, 115), while lowering HAS expression reduced tumor growth rates (57, 116–121). Similarly, hHyal overexpression is correlated with negative outcomes. In a variety of cancers, hHyal2 (122, 123), hHyal4 (124, 125), and PH-20 (126, 127) were all found to be overexpressed. Human Hyal1 is the most well studied member of the hHyal family, and its overexpression was found in prostate (22, 24), bladder (128, 129), colorectal (122), breast (130), bladder (131),

ovarian (132), pancreatic (133), and lung (134) cancers. Human Hyal1 overexpression accelerates prostate cancer by degrading extracellular HA to its LMW form, which alters the ECM thereby increasing motility, vesicle trafficking, membrane receptor turnover and changing stromal cell behavior (25, 105, 135–137). Conversely, stunting hHyal1 expression was shown to decrease tumor growth and motility in bladder cancer (137) and in breast cancer cells (138). Human Hyal1 quantification can also serve as a predictor for PCa disease progression after hormone deprivation therapy (139). It has been demonstrated that HA metabolism is coupled to cellular metabolism, with increased production of HA reprogramming the glycolytic and hexosamine biosynthetic pathways, promoting a cancerous phenotype (140, 141). Together, these findings suggest that HA is a key ECM component that can reorganize the ECM as well as cellular metabolism, according to cellular demands, ultimately increasing cancer progression.

There is abundant evidence that HA metabolism is key in cancer and other diseases, and while the field is continually investigating these links, how HA is fragmented in each condition remains a difficult question to answer. To that end, additional research and characterization needs to be done on the hHyals to understand their role in the dysregulated metabolism of HA that is a hallmark of cancer and other ailments. While most of the research has focused on hHyal1 and PH-20, far less is known about the other members of the hyaluronidase family. Different research groups have independently determined certain hHyal characteristics, but a comparative study of them has not yet been done. Investigation of these enzymes is a key step in understanding the dysregulated metabolism of HA that increases cancer progression.

Impact and research goals

Hyaluronidases and UDP-glucose dehydrogenase are both critical enzymes in normal cell function and are important in the progression of cancer. Elucidating the characteristics of these enzymes is necessary to gain a deeper understanding of how their dysregulation impacts ECM remodeling and tumor progression, and to facilitate drug development. Human UGDH activity can be regulated by small molecule scavengers of its products, such as 4MU (59–61), but where and how this interaction occurs is not yet known. Using X-ray crystallography, we aim to discover and model how a specific small peptide binds to and inhibits hUGDH. This interaction opens the door for increased understanding of hUGDH control and regulation, which is key in combating the progression of prostate cancer to a castration-resistant phenotype.

HA metabolism is a key component of ECM behavior, and the physiological roles of HA, hHAS and hHyal1 in inflammation, tumor progression and cancer metastasis have been thoroughly documented. Despite this knowledge, the hHyals have not been systematically characterized and the catalytic activity and substrate preference of each hHyal member remains a subject of debate amongst researcher groups. We aim to express, purify, and demonstrate the kinetic properties of hHyal1, 2, 3 and 4 to assist in the general understanding of HA metabolism. The insights gained from this work will assist future research efforts in learning about the complex mechanisms that govern HA degradation and could ultimately lead to leveraging or controlling the expression of hHyal proteins for therapeutic uses.

CHAPTER 2. Synthesis and Catalytic Activity of Human Hyaluronidases

Abstract

Hyaluronic acid (HA) and chondroitin sulfate (CS) are crucial components of the extracellular matrix and are involved in many important processes including joint lubrication, cellular growth, and division. In diseased states, such as cancer and inflammation, HA metabolism is dysregulated and can lead to worsening inflammation as well as increased cell motility and ultimately, metastasis. HA and CS are fragmented by the hyaluronidase (Hyal) family of proteins. The five human Hyal proteins (hHyal1-4, and hPH-20) are naturally expressed at different levels and have varying levels of catalytic activity with a preferred substrate. Although the importance of HA metabolism is well known, no group has yet systematically investigated and compared the activity of hHyals 1, 2, 3, and 4. Here, a system is described for the expression, purification, quantification, and catalytic measure of hHyal1-4. This system is adaptable and able to purify proteins with or without FLAG and / or poly-His epitopes. Following purification, the catalytic ability of each hHyal protein was evaluated using a colorimetric assay to show that at pH 4.0, hHyal1 efficiently degrades HA and CS, hHYAL2 breaks down CS and HA at a much slower rate than hHyal1, hHyal4 degrades CS only (to a lesser extent than hHyal1), and hHyals 3 does not cleave either HA or CS. This work will act as a standard for the catalytic ability of each hHyal and provide an expression and purification blueprint The expression and purification methods here will readily produce sufficient protein to completely characterize the hHyal proteins.

Introduction

As an essential component of the extracellular matrix (ECM), hyaluronic acid (HA) has many important physical functions including tissue lubrication, hydration, and cushioning, as well as the physiological roles of wound healing, inflammatory response, and motility (66–69). These key physiological functions mean that HA is a uniquely powerful structural and signaling molecule that impacts cell morphogenesis, growth, division, embryogenesis, tumorigenesis, and inflammation (72–78). Since delicate regulation of HA is necessary for proper cell and matrix function, altered HA metabolism results in a variety of ailments. HA and another glycosaminoglycan (GAG), chondroitin sulfate (CS), are catalytically degraded into smaller fragments by the hyaluronidase (Hyal) family of enzymes (66, 74, 79–81), which utilize a substrate-assisted mechanism to hydrolyze the β-1-4 linkage between N-acetylglucosamine and glucuronate in the sugar backbone (86–88). Humans express five different Hyal proteins (hHyal 1-4, and PH-20), with varying degrees of activity for HA and / or CS. Human Hyals are named as such because of their protein sequence homology, not necessarily because they have been shown to break HA chains. The most thoroughly studied member of this family is hHyal1, as it appears to be the hHyal primarily responsible for enzymatic HA degradation, outside of reproductive tissue.

Hyal1 is an efficient chondroitinase and hyaluronidase (87, 142, 143) that can rapidly cleave HA to a size of four or six sugars in length (144). Human Hyal1 is commonly associated with tumor biology, wound healing and lysosome function (104, 145, 146). Speculation remains regarding the catalytic competence of hHyal2, though it was shown to cleave high molecular weight (HMW) to 20 kDa fragments (147, 148). However, this activity may be dependent upon the expression of CD44, a transmembrane glycoprotein and receptor for HA, as well as

association with a cell surface proton pump (149). Human Hyal3 has no documented activity (150), but its overexpression was thought to amplify hHyal1 activity (151). Although hHyal4 is not able to degrade HA, it is known to fragment CS (152). Finally, PH-20 is expressed almost exclusively on the head of sperm to degrade HA to aid in egg fertilization (153, 154). Hyal2, Hyal4 and PH-20 are each attached to the cell by a glycosylphosphatidylinositol (GPI) anchor, which may be important in their respective physiological roles (93). Much is still not understood regarding the nuances of the hHyal family. The catalytic activity and substrate preferences of the hHyals have not been characterized, and different research groups determine catalytic rates in a different way that makes it difficult to reach broad conclusions regarding the characteristics of each member of this family.

The general role of hHyals in dysregulated HA metabolism is well established, but most work has focused on hHyal1 alone, while the roles and catalytic abilities of other hHyal proteins are unknown or conflicting. To add to this, different research groups have characterized the catalytic nature of a given hHyal using a method unique to that group. To aid in the research efforts of HA metabolism and specifically the role of hHyals, HEK293 suspension cells were used to express the hHyal of choice into the conditioned media, which were purified in a variety of ways. Activity is tested using chemical derivatization to colorimetrically quantify the number of reducing ends of a GAG, which increases as HA or CS is fragmented by Hyal (155–157). These research findings will assist in the continued efforts to understand Hyal mechanisms, expression patterns and their physiological role in normal and abnormal HA metabolism.

Materials and Methods

Site-directed mutagenesis

Sequencing of the hHyal2 plasmid revealed a K4N mutation. To correct the mutation by site-directed mutatgenesis, primers were designed using the Agilent online tool (https://www.agilent.com/store/primerDesignProgram.jsp) and the following sequences were ordered through IDT: (5'-gtggtgctgtgggcttgagctccataagcttgtc-3' and 5'-gacaagcttatggagctcaagcccacagcaccac-3'). The new DNA sequence was synthesized using Agilent's QuickChange thermal cycling protocol with KOD Hot Start DNA Polymerase (71086, Millipore). The thermal cycling protocol was done at three different annealing temperatures to increase the likelihood of getting a pure product: 66.9ºC, 65.2ºC and 62.5ºC. A *Dpn* 1 digestion (FD1704, Thermo Scientific) step was performed according to the manufacturer to remove the parent strand containing the undesired K4N mutation.

Protein transformation and transfection

Human HYAL plasmids used for this project are constructed in the pFLAG-CMV-3 vector (E6783, Sigma), and only hHYAL4 contains a polyhistidine tail. To direct the expressed protein into the media, the GPI anchor was removed where applicable (hHYAL2 and 4), and a preprotrypsin leader sequence was added upstream of the protein start.

Human HYAL plasmid constructs were used to transform DH5α max efficiency cells (18258012, Invitrogen). Cells were grown overnight at 37ºC on agarose plates containing ampicillin. Isolated colonies were selected and placed into a 5 mls of 31.0 g/L 2xYT broth plus 5 µl of 100 mg/ml ampicillin in a 37ºC, 120 rpm incubator for 8 hours. This was transferred to 50 ml of 31.0 g/L 2xYT broth media containing 50 µl of 100 mg/ml ampicillin, which was then incubated overnight at 37ºC, 120 rpm. DNA was isolated the next day by following the QIAGEN

Midiprep kit (12143, QIAGEN) instructions. DNA plasmid concentrations were determined by the DNA / RNA estimation program on the Cary 60 (G6860A, Agilent). Sequences were verified by Eton Bioscience Inc (Research Triangle Park, NC).

Soluble Expi293 cells were purchased from ThermoFisher as part of the Expi293 Expression System Kit (A14635-01, Gibco) and were maintained in a 30 ml suspension culture as directed by the manufacturer. Expi293 cells were seeded one day prior to transfection at 60 x 10^6 cells / flask. On the day of transfection, 75 x 10^6 cells were placed into a new flask, totaling 25.5 ml of media. Per flask, 30 µg of appropriate hHYAL plasmid DNA was added to 1.5 ml of Opti-MEM (ref#31985-062, Gibco), while in a separate tube, 81 µl of epifectamine 293 reagent was added to Opti-MEM media totaling 1.5 ml. The DNA and epifectamine solutions were mixed and incubated at room temperature for 20 minutes before adding to the cells and placed in an incubator at 37ºC, 5% CO_2 and 120 rpm. After 20 hours of incubation, 150 µl of Enhancer 1 and 1.5 ml of Enhancer 2 were added to the cell flask, totaling 30 ml.

Protein purification

Transfection flasks were removed from the incubator 6 days post-transfection and immediately centrifuged at 500 x g for 15 min at 4ºC (5810, Eppendorf); cells were discarded and the supernatant was treated with a half tablet of crushed protease inhibitor (ref#A32965, Thermo Scientific), then centrifuged at 15000 x g for 15 min at 4ºC (5810, Eppendorf). The supernatant was placed into SnakeSkin™ Dialysis Tubing, 10K MWCO (68100, Thermo Scientific) and dialyzed against 50 mM tris, pH 7.5, for 1-2 hours at room temperature, then overnight at 4ºC in 2 L fresh dialysis buffer before purification.

Human Hyal1 was purified by ammonium sulfate precipitation (ASP) and ion-exchange chromatography (IEC) as previously reported. Two flasks can be purified at once using this

method. Tris buffer (50 mM Tris, 5 mM EDTA) and ammonium sulfate (AS; 3.9 M ammonium sulfate in Tris buffer) solutions were made in preparation for ASP. Briefly, 10%, 20%, 30%, 40% and 100% AS saturation were achieved in 30 ml of Expi293 protein media containing hHyal1. After each AS addition, the solution stirred on ice for 10 minutes before centrifugation at 4^{o}C for 15 minutes at 15,000 x g (5810, Eppendorf), and the resulting protein pellet was resuspended in Tris buffer. The fractions containing hHyal1 were pooled and dialyzed for 1-2 hours at room temperature, then overnight at 4^{o}C.

Dialyzed protein was purified on the ÄKTA start system (29022094, Cytiva) using UNICORN start 1.0 and a 5 ml Nuvia Q strong ion exchange column (732-4741, BioRad) with a flow rate of 1 ml/min. Using the anion exchange program, the APS-purified hHyal1 protein solution was loaded, and the column was washed with 9 column volumes of buffer A. Flow through and wash fractions were collected. Protein was eluted with a gradient of buffer B (50 mM Tris, pH 7.5, plus 2 M NaCl, pH 7.5).

Human Hyal2 and 3 were purified by affinity chromatography using an ANTI-FLAG M2 resin (A2220, Sigma). Dialyzed hHyal transfection media was loaded onto immobilized ANTI-FLAG M2 resin and flow through was passed twice more over the column before collecting the flow through, wash and elution fractions. Resin preparation, column preparation, and protein elution were performed according to the manufacturer.

Human Hyal4 was purified by nickel affinity chromatography using the ÄKTA start system (29022094, Cytiva) with UNICORN start 1.0 and a charged Ni^{2+} 5 ml HisTrap column (cat#17525501, Cytiva). At a constant flow rate of 5 ml/min, the dialyzed protein solution was loaded onto the column and washed with 9 column volumes of buffer A (50 mM NaH_2PO_4, 500 mM NaCl, 10 mM Imidazole). Protein was eluted with an imidazole gradient in buffer B (50 mM

NaH_2PO_4, 500 mM NaCl, 250 mM Imidazole). Flow through, wash, and elution fractions were collected. Four transfection flasks were pooled for simultaneous purification using this method.

Further clean-up of hHyal4 was attempted by IEC using the 20 ml Q anion column on the ÄKTA start system (29022094, Cytiva) with UNICORN start 1.0. The isoelectric point of hHyal4 is 7.5, so pH 8.75 was chosen for purification. After loading the hHyal4 protein solution onto the column and washing with 20 column volumes of buffer A (50 mM Tris, pH 8.75), an increasing gradient of buffer B (50 mM Tris, 100 mM NaCl, pH 8.75) was used to elute the protein.

Selected eluted protein fractions were run on 10% SDS-PAGE gels for Coomassie staining and immunoblotting against the FLAG tag (see below) to detect protein in eluted fractions. Fractions with significant amounts of protein and small amounts of impurities were pooled, placed in SnakeSkin™ Dialysis Tubing, 10K MWCO (68100, Thermo Scientific), and dialyzed against 2 L dialysis buffer (50 mM tris, pH 7.5) for 1-2 hours at room temperature, then overnight at 4^{o}C in a fresh 2 L dialysis buffer. Purified and dialyzed hHyal proteins were concentrated using an Amicon Ultra-15 10K centrifugal filter (C7715, Millipore) unit according to the manufacturer's instructions, then the purified protein concentration was determined by the scan function at 280 nm on the Cary 60 (G6860A, Agilent). To visually observe protein purity, a small aliquot of protein was run on a 10% SDS-PAGE gel and inspected with Coomassie staining. Validated purified protein was flash frozen in liquid nitrogen and stored at −80°C.

Immunoblotting

Samples were denatured at 95^{o}C for 5 minutes prior to gel electrophoresis. All gels were made as 10% acrylamide SDS-PAGE gels and run for 1 hour and 10 minutes at 200 V and 15 mA (30 mA for 2 gels) in 1X running buffer. Transfer of proteins from the gel to a membrane

was accomplished with a 1X transfer buffer on ice at 100 V for 1 hour. While gently rocking, membrane blocking buffer (5% dry milk in 1X PBS) was placed on the membrane for 45 minutes at room temperature, then replaced with a primary antibody solution (5% dry milk in 1X PBS 0.1% Tween, plus 1:1000 mouse anti-FLAG (F3165, Sigma)) for 2 hours at room temperature, followed by four 5-minute washes with 1X PBS 0.1% Tween. Protected from light, secondary antibody solution (5% dry milk in 1X PBS 0.1% Tween, plus 1:15000 680 nm goat anti-mouse (925-68070, LICOR)) was added to the membrane for 45 minutes, followed by four additional 5-minute washes with 1X PBS 0.1% Tween. Then the blot was gently rinsed with distilled water and imaged using the Odyssey imaging instrument (9140, LICOR). SeeBlue™ Plus2 Pre-stained Protein Standard was used as a protein ladder (LC5925, Invitrogen).

Enzymatic activity analysis

To determine the catalytic activity of hHyal proteins with either CS or HA as a substrate, the Morgan-Elson assay was performed to detect reducing ends of GAGs, which become more abundant as catalysis occurs and can be colorimetrically measured at 585 nm (155, 156). The assay was carried out as described by Takahashi *et al.* (157) with minor modifications. In triplicate, a no enzyme control or hHyal protein solution (Hyal1: 0.1 µg/rxn; Hyal2, 3, 4: 1µg/rxn) were mixed with 10 different concentrations of substrate (200 µM – 0 µM, 61.8 kDa HA (HA40K-1, HAWORKS); 2.5 mg/ml – 0 mg/ml, avg 25 kDa CS (C6737-5G, Sigma)) in activity assay buffer (0.1M sodium formate, 0.15 M NaCl, pH 4.0) to a total volume of 65 µl. This was incubated in a 37°C water bath (Hyal1: 15 min; Hyal2, 3: 24 hours; Hyal4: 60 min) then boiled 5 min at 100°C to halt the reaction. A concentration gradient of standards (for HA: *N*-acetyl-d-glucosamine (A8625, Sigma); for CS: *N*-acetyl-d-galactosamine (A2795, Sigma)) were made and used to extrapolate available sugar reducing ends. To each sample and standard

tube containing 65 µl, 12.5 µl 0.8 M potassium tetraborate ($K_2B_4O_7 \cdot 4H_2O$) was added followed by a 5 min boil at 100°C. Then 375 µl 1X p-dimethylaminobenzaldehyde (DMAB) was added and the solutions were incubated for 20 minutes at 37°C. Samples were centrifuged at 14,000 rpm for 5 min, then 150 µl of each sample was pipetted into a 96-well plate and colorimetrically analyzed at 585 nm using the BioTek plate reader (8040036, BioTek). Data was imported into PRISM (GraphPad Software Inc., La Jolla, CA) and K_m and V_{max} were calculated by fitting to the Michaelis-Menten equation.

Results

Addition of pre-protrypsin and FLAG epitopes to hHyal1-4 facilitated secretion of the recombinant proteins from expi293 cells and subsequent detection, respectively. Protein expression varied significantly. Transfection of expi 293 cells with the hHyal1, 2, 3, and 4 plasmids produced an estimated 1.0, 0.1, 0.4 and 0.9 mg/ml of purified protein per flask, respectively.

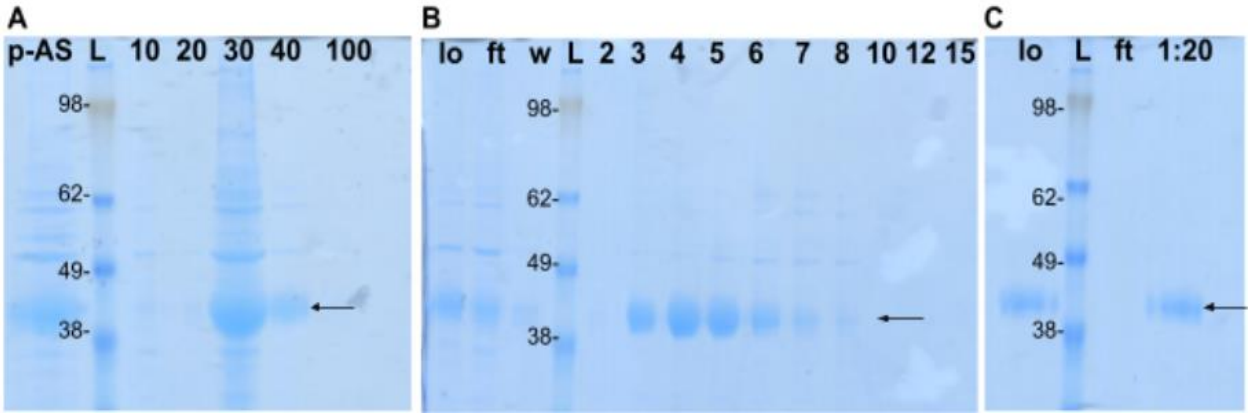

Figure 2 Human Hyal1 purification by ammonium sulfate precipitation (ASP), followed by ion-exchange chromatography (IEC). A) Coomassie stain of total protein before (p-ASP) and after ASP (numbers indicate ASP percentage). B) Coomassie stain of total protein and ASP-purified hHyal1 before and after IEC purification. C) Coomassie stain of IEC-purified hHyal1 after fractions 3, 4, 5, 6 were pooled and concentrated using the Amicon-15 centrifugation concentrator. The presence of hHyal1 is indicated with an arrow. Load (lo), flow through (ft), wash (w), ladder (L).

Ammonium sulfate precipitation (APS) is a common and effective method for protein purification. Increasing the concentration of highly charged ions to a solution will compete with water to bind with the protein, resulting in decreased solubility and increased protein precipitation (158). Human Hyal1was precipitated at 30% and 40% ammonium sulfate (Fig. 2A). These fractions were combined and dialyzed for IEC. After IEC, fractions 3-6 contained hHyal1 with little unwanted protein; fractions 7 and 8 contained hHyal1 and many other proteins and were discarded (Fig. 2B). Concentrated fractions were 95% pure (Fig. 2C).

Initial sequencing of the Hyal2 plasmid revealed a mutation at position 4 (K4N), which was reverted to the wildtype sequence using site-directed mutagenesis (SDM). After the thermal cycling protocol was used to amplify the corrected plasmid sequence, the reaction products were run on an agarose gel (Fig. 3A). Human Hyal2 was purified by immunoaffinity chromatography. Although not visible in a Coomassie stained gel (Fig. 3B), immunoblotting for the FLAG epitope revealed the presence of hHYAL2 in fraction 2 (Fig. 3C). Fractions 1 through 4 were pooled and

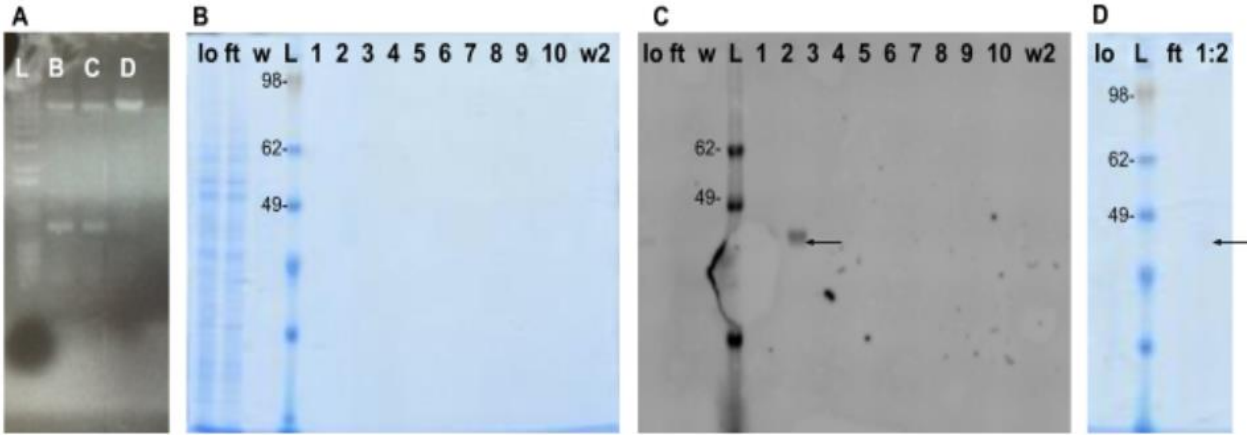

Figure 3 SDM and hHyal2 purification by 1 ml ANTI-FLAG resin. A) Site directed mutagenesis results of three different annealing temperatures (B: 66.9ºC, C: 65.2ºC, D: 62.5ºC). B) Coomassie staining of total protein before and after ANTI-FLAG purification, hHyal2 cannot be seen due to low protein expression. C) Immunoblotting for the hHyal2 FLAG epitope before and after ANTI-FLAG purification. D) Coomassie staining after fractions 1-4 were pooled and concentrated using Amicon-15 centrifugation concentrators, hHyal2 can be seen very faintly in the concentrated protein lane on the far right. The presence of hHyal2 is indicated with an arrow. Flow through (ft), wash (w), load (lo), ladder (L).

concentrated. Coomassie staining of the concentrated product showed an extremely faint Hyal2 product due to low protein expression (Fig. 3D).

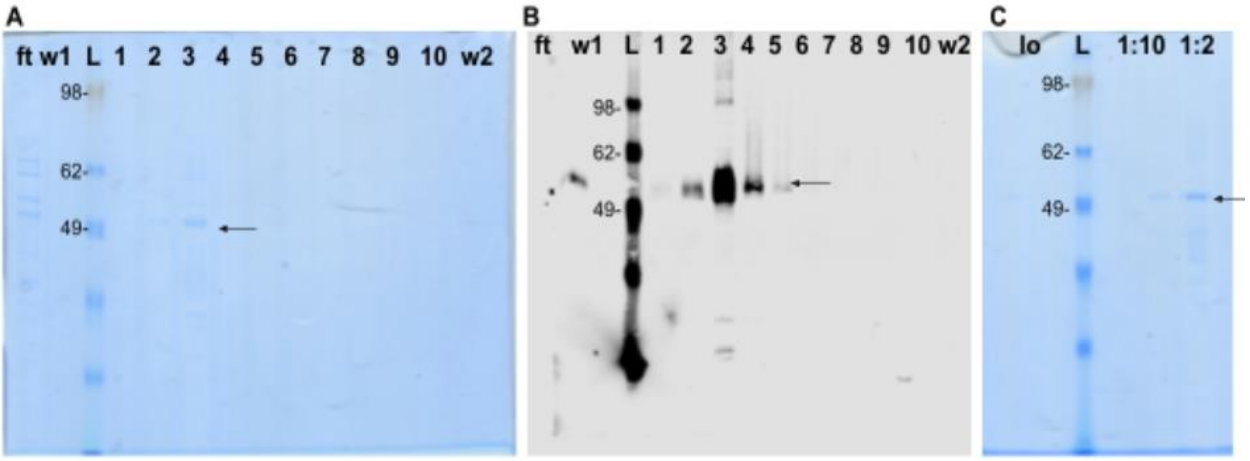

Figure 4 Human Hyal3 purification by 1 ml ANTI-FLAG resin. A) Coomassie staining of total protein before and after ANTI-FLAG purification. B) Immunoblotting for the hHyal3 FLAG epitope before and after ANTI-FLAG purification. D) Coomassie staining after fractions 2-5 were pooled and concentrated using Amicon-15 centrifugation concentrators. The presence of hHyal3 is indicated with an arrow. Flow through (ft), wash (w), load (lo), ladder (L).

Isolation of hHyal3 was also purified by immunoaffinity chromatography. Human Hyal3 appeared in fraction 3 on a Coomassie stained gel (Fig. 4A) and in fractions 2 through 5 by western blot analysis and detection of the FLAG epitope (Fig. 4B). Purity of the concentrated protein was confirmed (Fig. 4C).

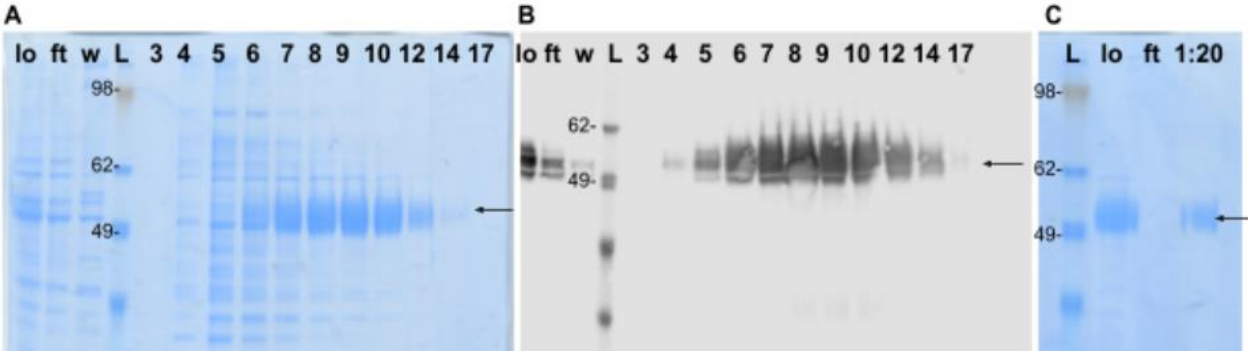

Figure 5 Human Hyal4 purification by 5 ml HisTrap protocol. A) Coomassie staining of total protein before and after HisTrap purification. B) Immunoblotting for the hHyal4 FLAG epitope before and after HisTrap purification. C) Coomassie staining after fractions 7-17 were pooled and concentrated using Amicon-15 centrifugation concentrators. The presence of hHyal4 is indicated with an arrow. Flow through (ft), wash (w), load (lo), ladder (L).

Purification of hHyal4 by nickel affinity chromatography was monitored by Coomassie staining and immunoblot detection of the FLAG epitope. Coomassie staining revealed a large amount of the total protein content eluted in fractions 4, 5, and 6; and an abundance of hHyal4 in fractions 6-12 (Fig. 5A). Immunoblotting of the FLAG tag confirmed the presence of hHyal4 in fractions 4-17 (Fig. 5B). Due to the high ratio of undesired protein to hHyal4 in fractions 4-6, fractions 7-17 were pooled for dialysis and concentration, which shows a large yield of pure hHyal4 when analyzed by Coomassie staining (Fig. 5C).

With the goal of creating enough high purity hHyal4 for future X-ray crystallography studies, 25 mg of hHyal4 protein was purified using the anion exchange Q column. After purification, a significant amount of total protein appeared to elute in fractions 8-20 (Fig. 6A), and the FLAG tagged hHyal4 protein was shown in fractions 6-27 (Fig. 6B). Despite the presence of impurities in fractions 10-20, fractions 6-27 were pooled for dialysis and concentrated the following day. The resulting Coomassie stain shows a large amount of concentrated Hyal4, as well as trace impurities (Fig. 6C). Despite a small batch of hHyal4 being

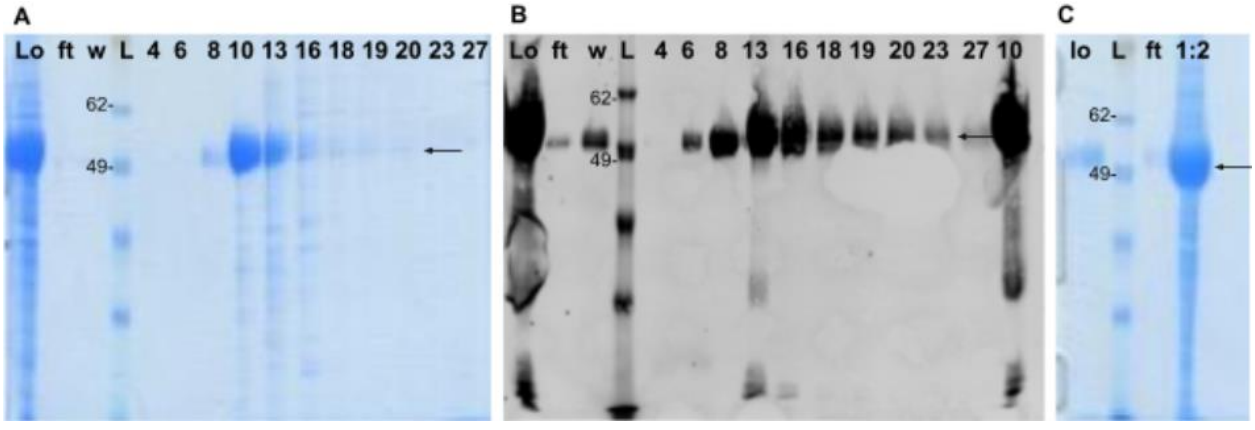

Figure 6 Human HYAL4 clean up by 20 ml Q column anion exchange protocol. 25 mg of purified hHYAL4 (by 5 ml HisTrap) were pooled, then purified. A) Coomassie staining of total protein before and after Q column anion exchange purification. B) Immunoblotting for the hHYAL4 FLAG epitope before and after Q column anion exchange purification. C) Coomassie staining after fractions 6-27 were pooled and concentrated using Amicon-15 centrifugation concentrators. The presence of hHYAL4 is indicated with an arrow. Flow through (ft), wash (w), load (lo), ladder (L).

used (5 mg) for an initial purification test (data not shown), this method was unsuccessful in removing impurities when loaded with 25 mg of protein.

Enzymatic activity of the purified hHyal enzymes were compared at pH 4.0. Incubation times and enzyme concentrations are summarized in Table 1. Despite significantly less protein per reaction, hHyal1 had the highest level of HA and CS activity. Activity of hHyal2 in hydrolysis of CS and HA was detectable but at much lower levels relative to that of hHyal1. As previously reported, hHyal4 only cleaved CS (at a rate between those of hHyal2 and hHyal1), and hHyal3 did not exhibit any catalytic activity (Fig. 5). Overexpression of murine Hyal3 was thought to augment Hyal1 activity in cultured cells (151). To see if there was increased activity when hHyal3 is combined with hHyal1, they were combined in 1:1 and 1:10 ratios (hHyal1: hHyal3) and tested against hHyal1 alone. No differences were observed in this experiment (data not shown), suggesting Hyal3 did not impact HA hydrolysis via hHyal1, as previously reported (151).

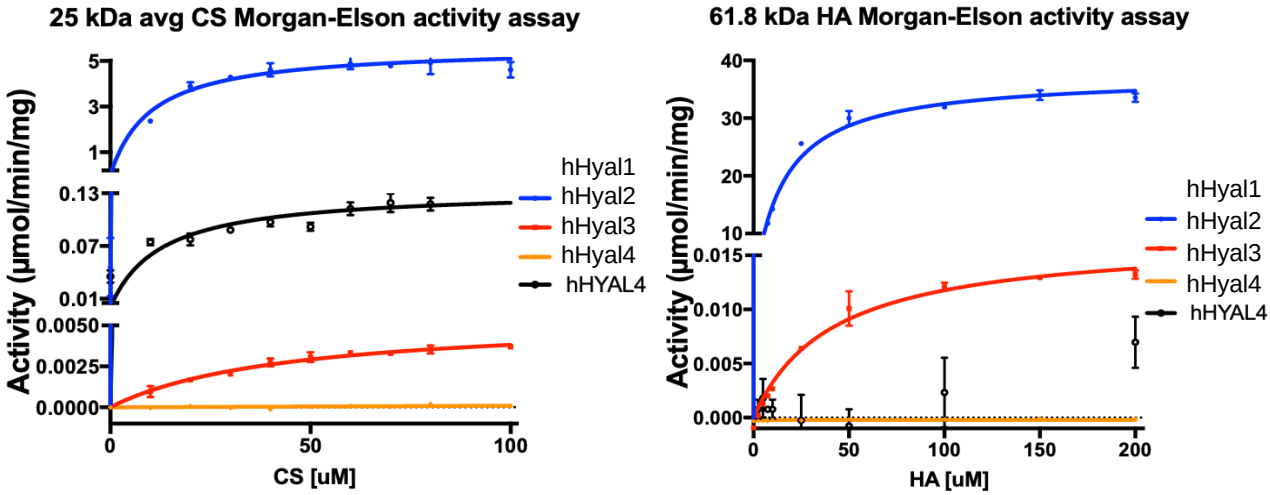

Figure 7 Human Hyal catalytic activity on 61.8 kDa hyaluronidase and 25 kDa (average size) chondroitin-sulfate, determined by the Morgan-Elson colorimetric activity assay. Briefly, hHyal is mixed with CS or HA in a pH 4.0 activity buffer and incubated at 37°C (15 minutes for hHyal1, 24 hours for hHyal2 and hHyal3, 60 minutes for hHyal4) then boiled to halt catalysis. DMAB and $K_2B_4O_7 \cdot 4H_2O$ were added for colorimetric quantification at 585 nm. hHyal1: 0.1 µg/rxn; hHyal2, 3, 4: 1µg/rxn.

Table 1 Catalytic activity of hHyals using the Morgan-Elson colorimetric assay, fit using the Michalis-Menten equation.

Enzyme	Conditions	Substrate (size)	Vmax (umol/min/mg)	Km (uM)
hHyal1	0.1 ug/rxn Inc 37C, 15 min	HA (61.8 kDa)	31.2 ± 0.476	15.2 ± 0.870
		CS (25 kDa)	5.68 ± 0.226	15.97 ± 2.404
hHyal2	1 ug/rxn Inc 37C, 24 hrs	HA (61.8 kDa)	0.017 ± 0.0006	41.31 ± 4.59
		CS (25 kDa)	0.0055 ± 0.00071	44.21 ± 13
hHyal3	1 ug/rxn Inc 37C, 24 hrs	HA (61.8 kDa)	---	---
		CS (25 kDa)	---	---
hHyal4	1 ug/rxn Inc 37C, 60 min	HA (61.8 kDa)	---	---
		CS (25 kDa)	0.1342 ± 0.0093	12.5 ± 3.76

Discussion

Purifying and expressing the hHyals is challenging and has hampered systematic analysis of this important family of proteins. Here, a dependable and reproducible system for the creation of hHyal proteins has been demonstrated, which can be readily applied for future studies in many ways. Expression and purification is easily achievable, although protein yields vary significantly for each hHyal. From 30 ml of conditioned media, mg quantities of purified hHyal1, 2, 3 and 4 were obtained.

Several points regarding expression and purification idiosyncrasies are noteworthy. Considering the nearly identical transfection procedure and high sequence homology, the difference in protein yields is surprising. One potential explanation is the possibility of having

altered folding or expression due to the removal of the GPI-attachment site in the hHYAL2 and hHYAL4 plasmids.

Another curious observation is the discrepancy between the sequence calculated weight of each hHyal core protein and its apparent molecular size by gel electrophoresis. The sequences of the hHYAL1, 2, 3, and 4 plasmids predict molecular weights of 48.4, 54.4, 47.6, and 51.4 kDa, respectively. When observed on gels, hHyal1, 2, 3, and 4 appear around 41, 44, 51, and 51, respectively. The difference between observed and expected weights is negligible for hHyal4 but a 10 kDa discrepancy exists for hHyal2. Differences could be due to self-cleaving or glycosylation events, which will be investigated further.

The purity of hHyal4 was not significantly improved by IEC, as shown in Fig. 5. Previously, using a much smaller load of hHyal4 and the same protocol and column, this method appeared to remove impurities (data not shown). It is possible that the column was overloaded. However, the manufacturer indicated a 25 mg column capacity. This will be further optimized and determined empirically.

Relative enzymatic activity was similar to previous reports, though there is inconsistency among them. Human Hyal1 is well accepted as a hyaluronidase and a chondroitinase; hHyal2 is a much less active hyaluronidase and a chondroitinase, hHyal3 does not appear to have any catalytic activity (150), and hHyal4 is a chondroitinase only. Previous research showed that hHyal1 displays optimal activity at pH 4.0 (142, 159), so all assays were performed at this pH, but it cannot be ruled out that other hHyal members may have pH activity profiles different to hHyal1, or that activity may be optimal with a different substrate size.

Discovering minor activity in hHyal2 was unexpected, and while the assay results certainly validate the activity of hHyal2 on both CS and HA at pH 4.0, this has only been tested

once, and will need further verification. Beyond increasing replications, a wide variety of experiments are needed to conclusively demonstrate the optimal catalytic activity of any hHyal.

Overall, it is interesting to speculate about possible functional redundancy among the hHyal family; perhaps each has an optimally sized substrate or expression condition or location. Many HA metabolism and hHyal questions remain unanswered and scientifically explaining these uncertainties could hint at the unique function of each hHyal. Further catalytic activity optimization as well as genomic, transcriptomic, and proteomic studies under different conditions and life development stages will accelerate greater understanding of their roles in cancer and ECM biology.

CHAPTER 3. Control and Inhibition of UDP-Glucose Dehydrogenase

Abstract

Human UDP-glucose dehydrogenase (hUGDH) is an essential enzyme consisting of a flexible trimer of dimers that is conformationally sensitive to substrate, product, and cofactor concentrations, and feedback inhibition. UGDH uses a NAD^+ cofactor to oxidize UDP-glucose to UDP-glucuronate, a substrate for three crucial cellular functions: glycosaminoglycan production, conversion to UDP-xylose for glycosaminoglycan and proteoglycan synthesis, and androgen glucuronidation. In humans, UGDH plays an important role in prostate cancer progression, with its overexpression marking an increased rate of tumor growth and motility. Therefore, hUGDH is a necessary target for drug development. Using a previously identified peptide sequence capable of inhibiting hUGDH, X-ray crystallographic analysis was performed on wild type hUGDH bound to the selected peptide inhibitor (P4). Solution of the structure revealed that addition of the peptide cased hUGDH to adopt an inactive protein conformation. This is supported by the orientation of key catalytic residues and the overall protein quaternary structure, which best reflects the previously reported structure of inactive, substrate-deficient hUGDH. The result of this work confirms the manner of UGDH inhibition and provides evidence of a potential drug that could be developed to limit the progression of prostate cancer by knocking down UGDH.

Introduction

As the sole enzyme capable of producing UDP-glucuronate (UDP-glcA), UGDH is uniquely poised to control the available substrate needed for three important cellular processes: HA synthesis, hormone glucuronidation, and proteoglycan (PG) synthesis. UDP-glcA is added to

drugs or toxins for excretion by glucuronosyltransferases (160–162), and this process promotes cancer therapy resistance (163–166). Additionally, UDP-glcA is a substrate for HA, which is excessively synthesized in cancers, promoting tumorigenesis (167–170). Therefore, controlling hUGDH activity or its ability to feed UDP-glcA into downstream pathways, is a potential therapeutic strategy.

UGDH expression is significantly elevated in human prostate cancer (18). Homogenous overexpression of UGDH within and adjacent to the tumor predicts biochemical recurrence following prostatectomy and the development of castration resistant phenotype (unpublished data). In cultured human prostate cancer cells, decreasing hUGDH expression results in increased androgen sensitivity (19, 26) and can restore sensitivity of castration resistant cells to the anti-androgen compound enzalutamide (27). Collectively, these results support the use of hUGDH as a biomarker in the diagnosis and appropriate treatment course of prostate cancer, and a potential drug target (18, 44). While the mechanism of hUGDH catalytic activity is well characterized, it is not known how hUGDH may be involved in directing UDP-glcA to a specific fate. It is possible that hUGDH acts as a sensor and prioritizes the use of newly created UDP-glcA. If so, hUGDH is not only an essential enzyme, but also one that determines cellular behavior and metabolism by influencing multiple pathways. Control and regulation of hUGDH represents a challenge with tremendous benefit, and while compounds such as 4MU, gallic acid and quercetin have been reported to antagonize UDP-GlcA production and even stunt breast cancer growth (58–61), the interaction between an inhibitor and hUGDH has not been visualized at an atomic level.

UGDH is optimally active as a dynamic quaternary assembly of three dimers in a toroid (28–30). As a hexamer, UGDH crystal structure determination has revealed three conformations,

corresponding to distinct catalytic states: an active E state, an inactive E* state, and a UDP-xylose inhibited EΩ state (30–39). In the EΩ state, UDP-xylose competes with UDP-glc for the active site and causes hUGDH inactivation and adoption of a horseshoe configuration (30, 31, 33). The E* state is prevalent in the absence of ligand and appears as a structural intermediate between the E and EΩ conformations (33). Thus, the shape of hUGDH is indicative of the functional state of the enzyme, and the creation of a compound that forces hUGDH to adopt the EΩ or E* state could be an important development in hUGDH therapeutics.

The discovery of UGDH-specific inhibitors has been facilitated by phage display, a screening technique in which bacteriophages display specific or randomized peptides fused to coat proteins (171), allowing us to select for peptides that tightly bind UGDH and alter its function (172–174). Phage display selection can be used to target a particular protein motif or to identify protein-protein interactions (175–177). Subsequently, the properties of the peptide can be used to direct high throughput screening (HTS) efforts to quickly identify promising inhibitory small molecules that are better drugs than peptides (170).

Previously, our lab used a codon-optimized *E. coli* expression vector to generate WT hUGDH (29). The phage display library fGWX10 was used to generate randomized 10-mer peptide sequences, with an estimated 10^{10} unique peptide sequences (178). Iterative rounds of selection were done to create a small list of promising peptide inhibitors, which were assessed using a phage ELISA assay (179). Human UGDH enzymatic activity (29, 38), thermal stability (29), trypsin susceptibility and inhibition studies were performed to further investigate the effects of the selected peptides. The highest performing 10-mer peptide (P4) displayed non-competitive inhibition with an $IC_{50} \sim 2$ μM (data not shown).

In this work, X-ray crystallography and structure determination of hUGDH in complex with P4 was used to examine the atomic-level contacts involved in the binding of hUGDH to P4. The data presented here can serve as a starting point to lead drug development efforts with the goal of controlling hUGDH and alleviating disease in those with overexpressed hUGDH.

Materials and Methods

Crystallization conditions

Successful crystallization of hUGDH:P4 occurred at 20°C using the sitting drop vapor diffusion method. A 40:1 WT hUGDH (5.47 mg/ml):P4 (9.75 mg/ml) solution was made prior to setting up a crystal tray. Highest quality crystals occurred with a reservoir solution of 0.1 - 0.2 M L-Proline with 6 - 7 % PEG 3350 and 0.1 M HEPES at pH 7.5 - 7.7; brought to 500 µl with ddH_2O. The 5 µL sitting drop was a mixture of 3 µL reservoir solution and 2 µL WT hUGHD:P4 solution. Crystals were screened in house and cryoprotected with a 2:1 mixture of reservoir solution: PEG400. All X-ray diffraction data was collected using the SER-CAT beamlines at the Advanced Photon Source (Argonne, IL). An approximately 3.50 Å resolution data set was collected on the 22-ID beamline using an Eiger 16M detector (Dektris). Data was processed using HKL-2000 (180). PDB entry 3ITK was used as a search model for molecular replacement in Phaser-MR from PHENIX (181). After performing simulated annealing on PHENIX (181), the resulting structure was manually rebuilt and improved with COOT (182) and refined using PHENIX (181). This process was repeated several times to ensure a quality resulting structure. Data collection and refinement statistics are shown in Table 2.

Table 2 hUGDH:P4 data collection and refinement statistics

	hUGDH:pept#4
Data collection	
Space Group	P212121
Unit cell dimensions (*a, b, c, β*)	88.2, 105.7, 365.0, 90.0°
Resolution Range	33.86-3.00
Completeness (%)	57.24
Redundancy	4.4 (4.1)
No. of reflections	37608
$I / \sigma(I)$	1.35
$CC_{1/2}$ [b]	91.9 (10.7)
R_{meas} [c] (%)	51.2 (379.5)
Refinement	
Resolution (Å)	3.00 (3.08-3.00)
R_{work} / R_{free}	0.177/0.287
R_{free} in highest resolution shell	39.05
Wilson *B*-factor	69.7
Stereochemical Ideality	
Bond lengths (Å^2)	0.009
Bond angles (°)	1.167°
φ,ψ Preferred region (%)	81.19
φ,ψ Additionally allowed (%)	11.53
φ,ψ Disallowed region (%)	7.28

Values in parentheses are for the highest-resolution shell (3.08-3.0 Å).

[b]CC1/2 is correlation between intensities from random half-data sets (183).

[c]R_{meas} is the redundancy-independent merging *R* factor (184).

Results

Human UGDH is a homohexamer that can exist in several conformations: active (E), inactive (E*) or UDP-xylose inhibited (EΩ). This transformation occurs in response to substrate and product concentrations. When compared to other hUGDH structures in the E, E* and EΩ from the protein data bank, the model presented in this work adopts a global conformation most like E* (Fig. 7A-C). Superimposing the different hUGDH forms revealed the conformations of key residues, which hint at a particular type of inhibition. E128 and E161 are key catalytic residues, and they adopt identical conformations in our structure and E* (Fig 7D). Together, these results indicate that P4 inhibits hUGDH by forcing it to adopt the conformation it would if

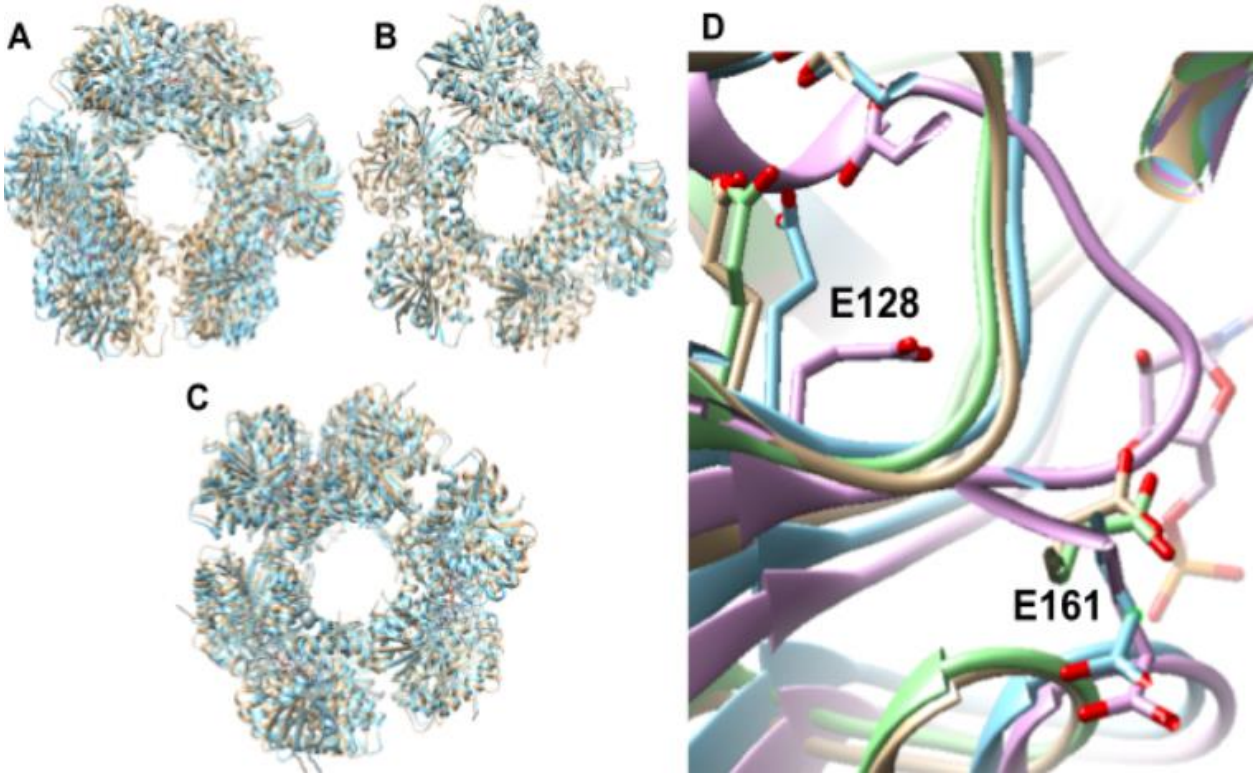

Figure 8 Global and residue-specific conformational changes in UGDH with the addition of peptide 4 as a functional inhibitor. A) Global alignment of UGDH:P4 (gold) versus EΩ UGDH (UDP-Xylose inhibited, blue). B) Global alignment of UGDH:P4 (gold) versus E* UGDH (inactive, blue). C) Global alignment of UGDH:P4 (gold) versus E UGDH (active, blue). D) Orientation comparisons of key catalytic glutamate residues in hUGDH (gold: UGDH:P4, purple: EΩ, green: E*, blue: E).

no substrate were present, therefore preventing catalysis. An alternative view is that the inhibitor preferentially binds to the E* conformation of hUGDH.

The findings detailed above are preliminary data, and deeper investigations are needed to confirm the relationship between hUGDH and P4. After data gathering at SER-CAT, processing with HKL-2000, and molecular replacement and refinement using PHENIX, the maximum resolution was found to be 3.00 Å, with a completeness of 57.7% and redundancy of 4.4. Because of the low resolution, only general conclusions can be drawn. Nonetheless, these findings suggest that UGDH adopts an inactive conformation when bound to P4.

Discussion

Human UGDH is a cancer biomarker and is functionally implicated in prostate tumor growth and therapeutic resistance (18). Our goal is to develop a specific small molecule inhibitor of UGDH that can be used as an adjuvant therapy to prevent or delay castration resistant recurrence. We previously identified a novel potential 10-mer peptide inhibitor of hUGDH (P4) that may be an effective lead compound for future small molecule screening. In this work, the peptide was co-crystallized with hUGDH and a molecular replacement solution was determined. Previous x-ray structure determination has revealed at least three different conformational states of hUGDH that correspond to the absence or presence of substrate and product, or an endogenous inhibitor: E (active), E* (inactive / substrate not available), or EΩ (UDP-xylose inhibited). Based on the position and orientation of well-known catalytic residues E128 and E161, we determined that hUGDH exists as E* when bound to P4. This indicates that P4 forces hUGDH to adopt an inactive shape, or that the P4:hUGDH complex is preferentially formed in the E* state. Additional testing is needed to determine if the peptide is cell permeable and

whether it decreases catalytic activity in a cellular context. Once the efficacy of P4 is confirmed, it can be used as a probe for small molecule screening. This small molecule will need to be validated as an effective modulator of hUGDH activity.

The discovery and production of a hUGDH small molecule inhibitor would dramatically shift the outlook for patients with prostate cancer, and although many more studies are needed, the work detailed here provides a sign of hope and promise moving forward in leveraging hUGDH to combat prostate cancer progression.

CHAPTER 4. Conclusions and Future Directions

We have described the expression, purification, and activity of the hHyal proteins, and provided structural insights into the binding characteristics and mechanisms of action of P4, a novel peptide inhibitor of hUGDH. Important advances made in this work are the standardization of consistent and effective protein expression and purification methods for human Hyal1-4, and a detailed preliminary comparison of the catalytic activities. The approaches described could be readily applied to express, purify and compare the more recently identified CEMIP and TMEM2 proteins, which have reported hyaluronidases activity at different optimal pH and different subcellular locations (94–96). In addition, site directed mutagenesis can be performed to alter key residues in less active hHyals, leading to better understanding of catalysis by trying to optimize activity. This approach would help identify structural, catalytic, and binding residues that are responsible for hHyals activity.

Although these results are practically useful, there remain many aspects of hHyal functions that have yet to be defined: the cellular, tissue specific and developmental expression patterns of the hHyals need to be analyzed, for example. Additionally, substrate and pH preference should be determined for each hHyal, including CEMIP and TMEM2.

To continue to understand the structural and kinetic characteristics of these important proteins, techniques such as surface plasmon resonance (SPR), isothermal titration calorimetry (ITC), and X-ray crystallography can be leveraged. SPR measures light reflected on a gold surface, which changes as a binding event occurs between an immobilized ligand and another protein flowing over the surface. SPR supports multiple applications, such as food safety, drug discovery, environment protection, and medical diagnostics (185). This application can be utilized to probe biomolecular interactions, such as protein-DNA or RNA, protein-protein, or

enzyme-substrate interactions (186, 187). SPR requires very little sample and can be used with a variety of linking methods (His tag, biotin tag, etc.) to quantitatively determine binding kinetics, competition, and thermodynamics. However, SPR is limited by orientation issues, tagging interference and protein conformation changes because of the experiment or binding to the chip. Preliminary SPR analysis of hHyal1 binding to biotinylated 5000 Da HA suggested a K_d = 1.2 μM at pH 4.65 (data not shown). However, this work could not be expanded upon because of technical and logistical issues. Therefore, these data are a foundation to be pursued and later adapted to the other hHyal proteins upon optimization of hHyal1.

ITC is another approach that could be used to probe the thermodynamics of a protein-protein interaction (PPI) by measuring heat changes resulting from the interaction. This sensitive and quantitative test can detail the stoichiometry, entropy, binding kinetics, and enthalpy in a PPI. Disadvantages include difficulties in measuring slow interactions and ensuring that the heat changes used to determine enthalpic constants derive exclusively from the PPI (188). One consideration for proper analysis by SPR and ITC is the need for the hHyal to exhibit binding but not catalysis. Catalysis would complicate data interpretation due to several factors to account for such as the number of binding sites on the substrate chain, increasing amounts of substrate fragments, and changing interactions between the substrate and water. Analyzing the catalytic reaction would be convoluted, and analysis models may not yet exist to accurately detail the catalytic reaction by ITC. To begin to analyze the binding interaction alone, a standard protocol should be tested at pH 4 - pH 7 in increments of 0.5. Human Hyal1, 2 and 4 are catalytically active at an acidic pH (the Morgan-Elson activity protocol is performed at pH 4.0, the optimal pH of hHyal1). It is not yet known whether binding occurs only when catalysis is possible or if binding can occur at a more neutral pH and the low pH is only needed for substrate cleavage.

Thus, enzymatic activity studies should be performed at a variety of pHs to determine the pH threshold of catalysis; then ITC and SPR can be performed just outside the catalytic pH range to try to find evidence of only binding. Using a different method to measure enzymatic activity, Hyal1 activity was highest at pH 3.5 and 4.0, and catalytically inactive for all substrates at pH 5.0 (142). Given this result, pH 5.0 should increase the likelihood of binding. An alternate approach would be to mutate a key catalytic residue, then observe binding at pH 4.0. Catalytic Hyal1 mutants E131Q and Y247F have been characterized by our group, but have not yet been studied by ITC or SPR.

To date, only hHyal1 has been entered into the protein data bank (PDB accession 2PE4), and this entry does not show binding to a substrate, nor residue mutations. Therefore, crystallization of the other hHyal proteins could shed light on the dramatic differences in enzymatic activity. Additional use of x-ray structure determination of each hHyal with its substrates would provide insights into mechanistic differences between the hHyal proteins. Several hHyal1 mutant structures should be determined to examine how the E131Q and Y202F mutants structurally impact the catalytic and binding ability of hHyal1, respectively. Furthermore, the substrate binding groove needs to be defined in the hHyals. To date, this has only been determined in bee venom Hyal, but there is low sequence homology between bee and hHyal. Understanding the interaction between HA or CS and a hHyal will provide additional clues about residues affecting catalysis among the hHyal family.

The development of a small molecule that can modulate hUGDH activity would be beneficial in combating prostate cancer and diseases resulting from an atypical ECM structure (since hUGDH provides ECM substrates). Here, it was shown that P4 binds to the E* state of hUGDH, bet we do not know if P4 forces hUGDH to adopt the inactive E* conformation, or if

E* preferentially binds to P4. Because the different conformations of hUGDH (E, E*, EΩ) are dependent cofactor, substrate, and product concentrations (31), P4 should be extensively characterized with various levels of available cofactor, substrate and UDP-xylose. Additionally, the binding affinity of P4 should be characterized, potentially with ITC. These studies will provide more details about the efficacy of P4 and should help in its eventual translation into a small molecule hUGDH modulator. These future compounds will need to be tested in a cellular context to assess cell permeability and confirm inhibition, also noting off-target effects. Structure determination should be repeated in co-crystals of hUGDH with potential small molecules based on P4, to understand the interaction and method of inhibition and to ensure hUGDH behaves similarly when bound to P4 or a future small molecule. Therefore, the evolution of P4 into a specific and potent inhibitor of hUGDH is an ongoing project.

Scientific biomedical research is a never-ending endeavor and motivated by the goals of furthering knowledge and improving human health. Our detailed comparative study for the production and characterization of the hHyals, and our insights into the mode of inhibition of a novel peptide inhibitor of hUGDH, provide a solid platform for future translational advances.

REFERENCES

1. Siegel, R. L., Miller, K. D., and Jemal, A. (2020) Cancer statistics, 2020. *CA: A Cancer Journal for Clinicians*. **70**, 7–30
2. Key Statistics for Prostate Cancer | Prostate Cancer Facts [online] https://www.cancer.org/cancer/prostate-cancer/about/key-statistics.html (Accessed December 30, 2020)
3. US Preventive Services Task Force (2018) Screening for Prostate Cancer: US Preventive Services Task Force Recommendation Statement. *JAMA*. **319**, 1901–1913
4. Fenton, J. J., Weyrich, M. S., Durbin, S., Liu, Y., Bang, H., and Melnikow, J. (2018) Prostate-Specific Antigen–Based Screening for Prostate Cancer: Evidence Report and Systematic Review for the US Preventive Services Task Force. *JAMA*. **319**, 1914–1931
5. Pernar, C. H., Ebot, E. M., Wilson, K. M., and Mucci, L. A. (2018) The Epidemiology of Prostate Cancer. *Cold Spring Harb Perspect Med*. 10.1101/cshperspect.a030361
6. Chu, K. C., Tarone, R. E., and Freeman, H. P. (2003) Trends in prostate cancer mortality among black men and white men in the United States. *Cancer*. **97**, 1507–1516
7. Etzioni, R., Gulati, R., Falcon, S., and Penson, D. F. (2008) Impact of PSA screening on the incidence of advanced stage prostate cancer in the United States: a surveillance modeling approach. *Med Decis Making*. **28**, 323–331
8. Draisma, G., Boer, R., Otto, S. J., van der Cruijsen, I. W., Damhuis, R. A. M., Schröder, F. H., and de Koning, H. J. (2003) Lead times and overdetection due to prostate-specific antigen screening: estimates from the European Randomized Study of Screening for Prostate Cancer. *J Natl Cancer Inst*. **95**, 868–878

9. Jemal, A., Center, M. M., DeSantis, C., and Ward, E. M. (2010) Global patterns of cancer incidence and mortality rates and trends. *Cancer Epidemiol Biomarkers Prev*. **19**, 1893–1907

10. Johansson, J.-E., Andrén, O., Andersson, S.-O., Dickman, P. W., Holmberg, L., Magnuson, A., and Adami, H.-O. (2004) Natural history of early, localized prostate cancer. *JAMA*. **291**, 2713–2719

11. Albertsen, P. C., Hanley, J. A., and Fine, J. (2005) 20-year outcomes following conservative management of clinically localized prostate cancer. *JAMA*. **293**, 2095–2101

12. Abeshouse, A., Ahn, J., Akbani, R., Ally, A., Amin, S., Andry, C. D., Annala, M., Aprikian, A., Armenia, J., Arora, A., Auman, J. T., Balasundaram, M., Balu, S., Barbieri, C. E., Bauer, T., Benz, C. C., Bergeron, A., Beroukhim, R., Berrios, M., Bivol, A., Bodenheimer, T., Boice, L., Bootwalla, M. S., Borges dos Reis, R., Boutros, P. C., Bowen, J., Bowlby, R., Boyd, J., Bradley, R. K., Breggia, A., Brimo, F., Bristow, C. A., Brooks, D., Broom, B. M., Bryce, A. H., Bubley, G., Burks, E., Butterfield, Y. S. N., Button, M., Canes, D., Carlotti, C. G., Carlsen, R., Carmel, M., Carroll, P. R., Carter, S. L., Cartun, R., Carver, B. S., Chan, J. M., Chang, M. T., Chen, Y., Cherniack, A. D., Chevalier, S., Chin, L., Cho, J., Chu, A., Chuah, E., Chudamani, S., Cibulskis, K., Ciriello, G., Clarke, A., Cooperberg, M. R., Corcoran, N. M., Costello, A. J., Cowan, J., Crain, D., Curley, E., David, K., Demchok, J. A., Demichelis, F., Dhalla, N., Dhir, R., Doueik, A., Drake, B., Dvinge, H., Dyakova, N., Felau, I., Ferguson, M. L., Frazer, S., Freedland, S., Fu, Y., Gabriel, S. B., Gao, J., Gardner, J., Gastier-Foster, J. M., Gehlenborg, N., Gerken, M., Gerstein, M. B., Getz, G., Godwin, A. K., Gopalan, A., Graefen, M., Graim, K., Gribbin, T., Guin, R., Gupta, M., Hadjipanayis, A., Haider, S., Hamel, L., Hayes, D. N., Heiman,

D. I., Hess, J., Hoadley, K. A., Holbrook, A. H., Holt, R. A., Holway, A., Hovens, C. M., Hoyle, A. P., Huang, M., Hutter, C. M., Ittmann, M., Iype, L., Jefferys, S. R., Jones, C. D., Jones, S. J. M., Juhl, H., Kahles, A., Kane, C. J., Kasaian, K., Kerger, M., Khurana, E., Kim, J., Klein, R. J., Kucherlapati, R., Lacombe, L., Ladanyi, M., Lai, P. H., Laird, P. W., Lander, E. S., Latour, M., Lawrence, M. S., Lau, K., LeBien, T., Lee, D., Lee, S., Lehmann, K.-V., Leraas, K. M., Leshchiner, I., Leung, R., Libertino, J. A., Lichtenberg, T. M., Lin, P., Linehan, W. M., Ling, S., Lippman, S. M., Liu, J., Liu, W., Lochovsky, L., Loda, M., Logothetis, C., Lolla, L., Longacre, T., Lu, Y., Luo, J., Ma, Y., Mahadeshwar, H. S., Mallery, D., Mariamidze, A., Marra, M. A., Mayo, M., McCall, S., McKercher, G., Meng, S., Mes-Masson, A.-M., Merino, M. J., Meyerson, M., Mieczkowski, P. A., Mills, G. B., Shaw, K. R. M., Minner, S., Moinzadeh, A., Moore, R. A., Morris, S., Morrison, C., Mose, L. E., Mungall, A. J., Murray, B. A., Myers, J. B., Naresh, R., Nelson, J., Nelson, M. A., Nelson, P. S., Newton, Y., Noble, M. S., Noushmehr, H., Nykter, M., Pantazi, A., Parfenov, M., Park, P. J., Parker, J. S., Paulauskis, J., Penny, R., Perou, C. M., Piché, A., Pihl, T., Pinto, P. A., Prandi, D., Protopopov, A., Ramirez, N. C., Rao, A., Rathmell, W. K., Rätsch, G., Ren, X., Reuter, V. E., Reynolds, S. M., Rhie, S. K., Rieger-Christ, K., Roach, J., Robertson, A. G., Robinson, B., Rubin, M. A., Saad, F., Sadeghi, S., Saksena, G., Saller, C., Salner, A., Sanchez-Vega, F., Sander, C., Sandusky, G., Sauter, G., Sboner, A., Scardino, P. T., Scarlata, E., Schein, J. E., Schlomm, T., Schmidt, L. S., Schultz, N., Schumacher, S. E., Seidman, J., Neder, L., Seth, S., Sharp, A., Shelton, C., Shelton, T., Shen, H., Shen, R., Sherman, M., Sheth, M., Shi, Y., Shih, J., Shmulevich, I., Simko, J., Simon, R., Simons, J. V., Sipahimalani, P., Skelly, T., Sofia, H. J., Soloway, M. G., Song, X., Sorcini, A., Sougnez, C., Stepa, S., Stewart, C., Stewart, J., Stuart, J. M., Sullivan, T.

B., Sun, C., Sun, H., Tam, A., Tan, D., Tang, J., Tarnuzzer, R., Tarvin, K., Taylor, B. S., Teebagy, P., Tenggara, I., Têtu, B., Tewari, A., Thiessen, N., Thompson, T., Thorne, L. B., Tirapelli, D. P., Tomlins, S. A., Trevisan, F. A., Troncoso, P., True, L. D., Tsourlakis, M. C., Tyekucheva, S., Van Allen, E., Van Den Berg, D. J., Veluvolu, U., Verhaak, R., Vocke, C. D., Voet, D., Wan, Y., Wang, Q., Wang, W., Wang, Z., Weinhold, N., Weinstein, J. N., Weisenberger, D. J., Wilkerson, M. D., Wise, L., Witte, J., Wu, C.-C., Wu, J., Wu, Y., Xu, A. W., Yadav, S. S., Yang, L., Yang, L., Yau, C., Ye, H., Yena, P., Zeng, T., Zenklusen, J. C., Zhang, H., Zhang, J., Zhang, J., Zhang, W., Zhong, Y., Zhu, K., and Zmuda, E. (2015) The Molecular Taxonomy of Primary Prostate Cancer. *Cell*. **163**, 1011–1025

13. Heinlein, C. A., and Chang, C. (2004) Androgen Receptor in Prostate Cancer. *Endocrine Reviews*. **25**, 276–308
14. Harris, W. P., Mostaghel, E. A., Nelson, P. S., and Montgomery, B. (2009) Androgen deprivation therapy: progress in understanding mechanisms of resistance and optimizing androgen depletion. *Nat Clin Pract Urol*. **6**, 76–85
15. Attar, R. M., Takimoto, C. H., and Gottardis, M. M. (2009) Castration-resistant prostate cancer: locking up the molecular escape routes. *Clin Cancer Res*. **15**, 3251–3255
16. Katzenwadel, A., and Wolf, P. (2015) Androgen deprivation of prostate cancer: Leading to a therapeutic dead end. *Cancer Lett*. **367**, 12–17
17. Spicer, A. P., Kaback, L. A., Smith, T. J., and Seldin, M. F. (1998) Molecular cloning and characterization of the human and mouse UDP-glucose dehydrogenase genes. *J Biol Chem*. **273**, 25117–25124

18. Huang, D., Casale, G. P., Tian, J., Lele, S. M., Pisarev, V. M., Simpson, M. A., and Hemstreet, G. P. (2010) Udp-glucose dehydrogenase as a novel field-specific candidate biomarker of prostate cancer. *Int J Cancer*. **126**, 315–327

19. Wei, Q., Galbenus, R., Raza, A., Cerny, R. L., and Simpson, M. A. (2009) Androgen-stimulated UDP-glucose dehydrogenase expression limits prostate androgen availability without impacting hyaluronan levels. *Cancer Res*. **69**, 2332–2339

20. Lokeshwar, V. B., Rubinowicz, D., Schroeder, G. L., Forgacs, E., Minna, J. D., Block, N. L., Nadji, M., and Lokeshwar, B. L. (2001) Stromal and epithelial expression of tumor markers hyaluronic acid and HYAL1 hyaluronidase in prostate cancer. *J Biol Chem*. **276**, 11922–11932

21. Ekici, S., Cerwinka, W. H., Duncan, R., Gomez, P., Civantos, F., Soloway, M. S., and Lokeshwar, V. B. (2004) Comparison of the prognostic potential of hyaluronic acid, hyaluronidase (HYAL-1), CD44v6 and microvessel density for prostate cancer. *Int J Cancer*. **112**, 121–129

22. Posey, J. T., Soloway, M. S., Ekici, S., Sofer, M., Civantos, F., Duncan, R. C., and Lokeshwar, V. B. (2003) Evaluation of the prognostic potential of hyaluronic acid and hyaluronidase (HYAL1) for prostate cancer. *Cancer Res*. **63**, 2638–2644

23. Aaltomaa, S., Lipponen, P., Tammi, R., Tammi, M., Viitanen, J., Kankkunen, J.-P., and Kosma, V.-M. (2002) Strong Stromal Hyaluronan Expression Is Associated with PSA Recurrence in Local Prostate Cancer. *Urol Int*. **69**, 266–272

24. Simpson, M. A. (2006) Concurrent Expression of Hyaluronan Biosynthetic and Processing Enzymes Promotes Growth and Vascularization of Prostate Tumors in Mice. *Am J Pathol*. **169**, 247–257

25. Bharadwaj, A. G., Kovar, J. L., Loughman, E., Elowsky, C., Oakley, G. G., and Simpson, M. A. (2009) Spontaneous metastasis of prostate cancer is promoted by excess hyaluronan synthesis and processing. *Am J Pathol*. **174**, 1027–1036

26. Zimmer, B. M., Howell, M. E., Wei, Q., Ma, L., Romsdahl, T., Loughman, E. G., Markham, J. E., Seravalli, J., Barycki, J. J., and Simpson, M. A. (2016) Loss of exogenous androgen dependence by prostate tumor cells is associated with elevated glucuronidation potential. *Horm Cancer*. **7**, 260–271

27. Zimmer, B. M., Barycki, J. J., and Simpson, M. A. (2021) Integration of Sugar Metabolism and Proteoglycan Synthesis by UDP-glucose Dehydrogenase. *J Histochem Cytochem.* **69**, 13–23

28. Campbell, R. E., Mosimann, S. C., van De Rijn, I., Tanner, M. E., and Strynadka, N. C. (2000) The first structure of UDP-glucose dehydrogenase reveals the catalytic residues necessary for the two-fold oxidation. *Biochemistry*. **39**, 7012–7023

29. Hyde, A. S., Thelen, A. M., Barycki, J. J., and Simpson, M. A. (2013) UDP-glucose Dehydrogenase Activity and Optimal Downstream Cellular Function Require Dynamic Reorganization at the Dimer-Dimer Subunit Interfaces. *J. Biol. Chem.* **288**, 35049–35057

30. Kadirvelraj, R., Sennett, N. C., Polizzi, S. J., Weitzel, S., and Wood, Z. A. (2011) Role of Packing Defects in the Evolution of Allostery and Induced Fit in Human UDP-Glucose Dehydrogenase. *Biochemistry*. **50**, 5780–5789

31. Beattie, N. R., Pioso, B. J., Sidlo, A. M., Keul, N. D., and Wood, Z. A. (2018) Hysteresis and Allostery in Human UDP-Glucose Dehydrogenase Require a Flexible Protein Core. *Biochemistry*. **57**, 6848–6859

32. Kadirvelraj, R., Sennett, N. C., Custer, G. S., Phillips, R. S., and Wood, Z. A. (2013) Hysteresis and Negative Cooperativity in Human UDP-Glucose Dehydrogenase. *Biochemistry*. **52**, 1456–1465

33. Kadirvelraj, R., Custer, G. S., Keul, N. D., Sennett, N. C., Sidlo, A. M., Walsh, R. M., and Wood, Z. A. (2014) Hysteresis in Human UDP-Glucose Dehydrogenase Is Due to a Restrained Hexameric Structure That Favors Feedback Inhibition. *Biochemistry*. **53**, 8043–8051

34. Sennett, N. C., Kadirvelraj, R., and Wood, Z. A. (2012) Cofactor Binding Triggers a Molecular Switch To Allosterically Activate Human UDP-α-d-glucose 6-Dehydrogenase. *Biochemistry*. **51**, 9364–9374

35. Sennett, N. C., Kadirvelraj, R., and Wood, Z. A. (2011) Conformational Flexibility in the Allosteric Regulation of Human UDP-α-d-Glucose 6-Dehydrogenase. *Biochemistry*. **50**, 9651–9663

36. Easley, K. E., Sommer, B. J., Boanca, G., Barycki, J. J., and Simpson, M. A. (2007) Characterization of Human UDP-Glucose Dehydrogenase Reveals Critical Catalytic Roles for Lysine 220 and Aspartate 280. *Biochemistry*. **46**, 369–378

37. Egger, S., Chaikuad, A., Klimacek, M., Kavanagh, K. L., Oppermann, U., and Nidetzky, B. (2012) Structural and Kinetic Evidence That Catalytic Reaction of Human UDP-glucose 6-Dehydrogenase Involves Covalent Thiohemiacetal and Thioester Enzyme Intermediates. *J. Biol. Chem.* **287**, 2119–2129

38. Sommer, B. J., Barycki, J. J., and Simpson, M. A. (2004) Characterization of Human UDP-glucose Dehydrogenase CYS-276 IS REQUIRED FOR THE SECOND OF TWO SUCCESSIVE OXIDATIONS. *J. Biol. Chem.* **279**, 23590–23596

39. Keul, N. D., Oruganty, K., Schaper Bergman, E. T., Beattie, N. R., McDonald, W. E., Kadirvelraj, R., Gross, M. L., Phillips, R. S., Harvey, S. C., and Wood, Z. A. (2018) The entropic force generated by intrinsically disordered segments tunes protein function. *Nature*. **563**, 584–588

40. Grady, G., Thelen, A., Albers, J., Ju, T., Guo, J., Barycki, J. J., and Simpson, M. A. (2016) Inhibiting Hexamer Disassembly of Human UDP-Glucose Dehydrogenase by Photoactivated Amino Acid Cross-Linking. *Biochemistry*. **55**, 3157–3164

41. Hyde, A. S., Farmer, E. L., Easley, K. E., Lammeren, K. van, Christoffels, V. M., Barycki, J. J., Bakkers, J., and Simpson, M. A. (2012) UDP-glucose Dehydrogenase Polymorphisms from Patients with Congenital Heart Valve Defects Disrupt Enzyme Stability and Quaternary Assembly. *J. Biol. Chem.* **287**, 32708–32716

42. Alhamoudi, K. M., Bhat, J., Nashabat, M., Alharbi, M., Alyafee, Y., Asiri, A., Umair, M., and Alfadhel, M. (2020) A Missense Mutation in the UGDH Gene Is Associated With Developmental Delay and Axial Hypotonia. *Front. Pediatr.* 10.3389/fped.2020.00071

43. Hengel, H., Bosso-Lefèvre, C., Grady, G., Szenker-Ravi, E., Li, H., Pierce, S., Lebigot, É., Tan, T.-T., Eio, M. Y., Narayanan, G., Utami, K. H., Yau, M., Handal, N., Deigendesch, W., Keimer, R., Marzouqa, H. M., Gunay-Aygun, M., Muriello, M. J., Verhelst, H., Weckhuysen, S., Mahida, S., Naidu, S., Thomas, T. G., Lim, J. Y., Tan, E. S., Haye, D., Willemsen, M. A. A. P., Oegema, R., Mitchell, W. G., Pierson, T. M., Andrews, M. V., Willing, M. C., Rodan, L. H., Barakat, T. S., van Slegtenhorst, M., Gavrilova, R. H., Martinelli, D., Gilboa, T., Tamim, A. M., Hashem, M. O., AlSayed, M. D., Abdulrahim, M. M., Al-Owain, M., Awaji, A., Mahmoud, A. A. H., Faqeih, E. A., Asmari, A. A., Algain, S. M., Jad, L. A., Aldhalaan, H. M., Helbig, I., Koolen, D. A., Riess, A.,

Kraegeloh-Mann, I., Bauer, P., Gulsuner, S., Stamberger, H., Ng, A. Y. J., Tang, S., Tohari, S., Keren, B., Schultz-Rogers, L. E., Klee, E. W., Barresi, S., Tartaglia, M., Mor-Shaked, H., Maddirevula, S., Begtrup, A., Telegrafi, A., Pfundt, R., Schüle, R., Ciruna, B., Bonnard, C., Pouladi, M. A., Stewart, J. C., Claridge-Chang, A., Lefeber, D. J., Alkuraya, F. S., Mathuru, A. S., Venkatesh, B., Barycki, J. J., Simpson, M. A., Jamuar, S. S., Schöls, L., and Reversade, B. (2020) Loss-of-function mutations in UDP-Glucose 6-Dehydrogenase cause recessive developmental epileptic encephalopathy. *Nature Communications*. **11**, 595

44. Egger, S., Chaikuad, A., Kavanagh, K. L., Oppermann, U., and Nidetzky, B. (2010) UDP-glucose dehydrogenase: structure and function of a potential drug target. *Biochem Soc Trans.* **38**, 1378–1385

45. Chen, J., and Yang, S. (2019) Catalytic mechanism of UDP-glucose dehydrogenase. *Biochemical Society Transactions*. **47**, 945–955

46. Campbell, R. E., Sala, R. F., van de Rijn, I., and Tanner, M. E. (1997) Properties and kinetic analysis of UDP-glucose dehydrogenase from group A streptococci. Irreversible inhibition by UDP-chloroacetol. *J Biol Chem*. **272**, 3416–3422

47. Ge, X., Penney, L. C., van de Rijn, I., and Tanner, M. E. (2004) Active site residues and mechanism of UDP-glucose dehydrogenase. *Eur J Biochem*. **271**, 14–22

48. Ordman, A. B., and Kirkwood, S. (1977) Mechanism of action of uridine diphoglucose dehydrogenase. Evidence for an essential lysine residue at the active site. *J Biol Chem*. **252**, 1320–1326

49. Ordman, A. B., and Kirkwood, S. (1977) Udpglucose dehydrogenase Kinetics and their mechanistic implications. *Biochimica et Biophysica Acta (BBA) - Enzymology*. **481**, 25–32

50. Ge, X., Campbell, R. E., van de Rijn, I., and Tanner, M. E. (1998) Covalent Adduct Formation with a Mutated Enzyme: Evidence for a Thioester Intermediate in the Reaction Catalyzed by UDP-Glucose Dehydrogenase. *J. Am. Chem. Soc.* **120**, 6613–6614

51. Chen, J., Yu, Y., Gao, J., and Yang, S. (2019) UDP-glucose Dehydrogenase: The First-step Oxidation Is an NAD+-dependent Bimolecular Nucleophilic Substitution Reaction (SN2). *Int J Biol Sci.* **15**, 341–350

52. Anttila, M. A., Tammi, R. H., Tammi, M. I., Syrjänen, K. J., Saarikoski, S. V., and Kosma, V. M. (2000) High levels of stromal hyaluronan predict poor disease outcome in epithelial ovarian cancer. *Cancer Res*. **60**, 150–155

53. Auvinen, P., Tammi, R., Parkkinen, J., Tammi, M., Agren, U., Johansson, R., Hirvikoski, P., Eskelinen, M., and Kosma, V. M. (2000) Hyaluronan in peritumoral stroma and malignant cells associates with breast cancer spreading and predicts survival. *Am J Pathol.* **156**, 529–536

54. Ropponen, K., Tammi, M., Parkkinen, J., Eskelinen, M., Tammi, R., Lipponen, P., Agren, U., Alhava, E., and Kosma, V. M. (1998) Tumor cell-associated hyaluronan as an unfavorable prognostic factor in colorectal cancer. *Cancer Res*. **58**, 342–347

55. Tammi, R. H., Kultti, A., Kosma, V.-M., Pirinen, R., Auvinen, P., and Tammi, M. I. (2008) Hyaluronan in human tumors: pathobiological and prognostic messages from cell-associated and stromal hyaluronan. *Semin Cancer Biol*. **18**, 288–295

56. Huh, J.-W., Choi, M.-M., Yang, S.-J., Yoon, S. Y., Choi, S. Y., and Cho, S.-W. (2005) Inhibition of Human UDP-Glucose Dehydrogenase Expression Using siRNA Expression Vector in Breast Cancer Cells. *Biotechnol Lett*. **27**, 1229–1232

57. Simpson, M. A., Wilson, C. M., and McCarthy, J. B. (2002) Inhibition of Prostate Tumor Cell Hyaluronan Synthesis Impairs Subcutaneous Growth and Vascularization in Immunocompromised Mice. *Am J Pathol*. **161**, 849–857

58. Hwang, E. Y., Huh, J.-W., Choi, M.-M., Choi, S. Y., Hong, H.-N., and Cho, S.-W. (2008) Inhibitory effects of gallic acid and quercetin on UDP-glucose dehydrogenase activity. *FEBS Lett.* **582**, 3793–3797

59. Kultti, A., Pasonen-Seppänen, S., Jauhiainen, M., Rilla, K. J., Kärnä, R., Pyöriä, E., Tammi, R. H., and Tammi, M. I. (2009) 4-Methylumbelliferone inhibits hyaluronan synthesis by depletion of cellular UDP-glucuronic acid and downregulation of hyaluronan synthase 2 and 3. *Exp Cell Res*. **315**, 1914–1923

60. Arnold, J. M., Gu, F., Ambati, C. R., Rasaily, U., Ramirez-Pena, E., Joseph, R., Manikkam, M., San Martin, R., Charles, C., Pan, Y., Chatterjee, S. S., Den Hollander, P., Zhang, W., Nagi, C., Sikora, A. G., Rowley, D., Putluri, N., Zhang, X. H.-F., Karanam, B., Mani, S. A., and Sreekumar, A. (2020) UDP-glucose 6-dehydrogenase regulates hyaluronic acid production and promotes breast cancer progression. *Oncogene*. **39**, 3089–3101

61. Nagase, H., Kudo, D., Suto, A., Yoshida, E., Suto, S., Negishi, M., Kakizaki, I., and Hakamada, K. (2017) 4-Methylumbelliferone Suppresses Hyaluronan Synthesis and Tumor Progression in SCID Mice Intra-abdominally Inoculated With Pancreatic Cancer Cells. *Pancreas*. **46**, 190–197

62. Weissmann, B., and Meyer, K. (1954) The Structure of Hyalobiuronic Acid and of Hyaluronic Acid from Umbilical Cord [1,2]. *J. Am. Chem. Soc.* **76**, 1753–1757

63. Laurent, T. C., and Fraser, J. R. (1992) Hyaluronan. *FASEB J.* **6**, 2397–2404

64. Monslow, J., Govindaraju, P., and Puré, E. (2015) Hyaluronan – A Functional and Structural Sweet Spot in the Tissue Microenvironment. *Front. Immunol.* 10.3389/fimmu.2015.00231

65. Kobayashi, T., Chanmee, T., and Itano, N. (2020) Hyaluronan: Metabolism and Function. *Biomolecules*. 10.3390/biom10111525

66. Fraser, J. R., Laurent, T. C., and Laurent, U. B. (1997) Hyaluronan: its nature, distribution, functions and turnover. *J Intern Med.* **242**, 27–33

67. Pinkus, H., and Perry, E. T. (1953) The influence of hyaluronic acid and other substances on tensile strength of healing wounds. *J Invest Dermatol*. **21**, 365–374

68. Ogston, A. G., and Stanier, J. E. (1953) The physiological function of hyaluronic acid in synovial fluid; viscous, elastic and lubricant properties. *J Physiol*. **119**, 244–252

69. Meyer, K. (1947) The biological significance of hyaluronic acid and hyaluronidase. *Physiological reviews*. 10.1152/PHYSREV.1947.27.3.335

70. Viola, M., Vigetti, D., Genasetti, A., Rizzi, M., Karousou, E., Moretto, P., Clerici, M., Bartolini, B., Pallotti, F., De Luca, G., and Passi, A. (2008) Molecular control of the hyaluronan biosynthesis. *Connect Tissue Res*. **49**, 111–114

71. Turley, E. A., Noble, P. W., and Bourguignon, L. Y. W. (2002) Signaling properties of hyaluronan receptors. *J Biol Chem*. **277**, 4589–4592

72. Tavianatou, A. G., Caon, I., Franchi, M., Piperigkou, Z., Galesso, D., and Karamanos, N. K. (2019) Hyaluronan: molecular size-dependent signaling and biological functions in inflammation and cancer. *FEBS J*. **286**, 2883–2908

73. Chanmee, T., Ontong, P., Kimata, K., and Itano, N. (2015) Key Roles of Hyaluronan and Its CD44 Receptor in the Stemness and Survival of Cancer Stem Cells. *Front. Oncol.* 10.3389/fonc.2015.00180

74. Heldin, P., Basu, K., Olofsson, B., Porsch, H., Kozlova, I., and Kahata, K. (2013) Deregulation of hyaluronan synthesis, degradation and binding promotes breast cancer. *The Journal of Biochemistry*. **154**, 395–408

75. Toole, B. P. (2004) Hyaluronan: from extracellular glue to pericellular cue. *Nature Reviews Cancer*. **4**, 528–539

76. Spicer, A. P., and Tien, J. Y. L. (2004) Hyaluronan and morphogenesis. *Birth Defects Research Part C: Embryo Today: Reviews*. **72**, 89–108

77. Knudson, C. B., and Toole, B. P. (1985) Changes in the pericellular matrix during differentiation of limb bud mesoderm. *Dev Biol.* **112**, 308–318

78. Tammi, R., Pasonen-Seppänen, S., Kolehmainen, E., and Tammi, M. (2005) Hyaluronan Synthase Induction and Hyaluronan Accumulation in Mouse Epidermis Following Skin Injury. *Journal of Investigative Dermatology*. **124**, 898–905

79. Girish, K. S., and Kemparaju, K. (2007) The magic glue hyaluronan and its eraser hyaluronidase: a biological overview. *Life Sci*. **80**, 1921–1943

80. Heldin, P., Lin, C.-Y., Kolliopoulos, C., Chen, Y.-H., and Skandalis, S. S. (2019) Regulation of hyaluronan biosynthesis and clinical impact of excessive hyaluronan production. *Matrix Biology*. **78–79**, 100–117

81. Erickson, M., and Stern, R. (2011) Chain Gangs: New Aspects of Hyaluronan Metabolism. *Biochemistry Research International*. **2012**, e893947

82. Stern, R., Kogan, G., Jedrzejas, M. J., and Šoltés, L. (2007) The many ways to cleave hyaluronan. *Biotechnology Advances*. **25**, 537–557

83. Soltés, L., Kogan, G., Stankovska, M., Mendichi, R., Rychlý, J., Schiller, J., and Gemeiner, P. (2007) Degradation of high-molar-mass hyaluronan and characterization of fragments. *Biomacromolecules*. **8**, 2697–2705

84. Bates, E. J., Harper, G. S., Lowther, D. A., and Preston, B. N. (1984) Effect of oxygen-derived reactive species on cartilage proteoglycan-hyaluronate aggregates. *Biochem Int*. **8**, 629–637

85. McNeil, J. D., Wiebkin, O. W., Betts, W. H., and Cleland, L. G. (1985) Depolymerisation products of hyaluronic acid after exposure to oxygen-derived free radicals. *Ann Rheum Dis*. **44**, 780–789

86. Jiang, D., Liang, J., and Noble, P. W. (2007) Hyaluronan in tissue injury and repair. *Annu Rev Cell Dev Biol*. **23**, 435–461

87. Zhang, L., Bharadwaj, A. G., Casper, A., Barkley, J., Barycki, J. J., and Simpson, M. A. (2009) Hyaluronidase Activity of Human Hyal1 Requires Active Site Acidic and Tyrosine Residues. *J. Biol. Chem.* **284**, 9433–9442

88. Wang, W., Wang, J., and Li, F. (2017) Hyaluronidase and Chondroitinase. in *Protein Reviews: Volume 17* (Atassi, M. Z. ed), pp. 75–87, Advances in Experimental Medicine and Biology, Springer, Singapore, 10.1007/5584_2016_54

89. Klecker, C., and Nair, L. S. (2017) Chapter 13 - Matrix Chemistry Controlling Stem Cell Behavior. in *Biology and Engineering of Stem Cell Niches* (Vishwakarma, A., and Karp, J. M. eds), pp. 195–213, Academic Press, Boston, 10.1016/B978-0-12-802734-9.00013-5

90. Baeurle, S. A., Kiselev, M. G., Makarova, E. S., and Nogovitsin, E. A. (2009) Effect of the counterion behavior on the frictional–compressive properties of chondroitin sulfate solutions. *Polymer*. **50**, 1805–1813

91. Singh, J. A., Noorbaloochi, S., MacDonald, R., and Maxwell, L. J. (2015) Chondroitin for osteoarthritis. *Cochrane Database Syst Rev*. **1**, CD005614

92. Monfort, J., Pelletier, J.-P., Garcia-Giralt, N., and Martel-Pelletier, J. (2008) Biochemical basis of the effect of chondroitin sulphate on osteoarthritis articular tissues. *Annals of the Rheumatic Diseases*. **67**, 735–740

93. Stern, R., and Jedrzejas, M. J. (2006) Hyaluronidases: their genomics, structures, and mechanisms of action. *Chem Rev*. **106**, 818–839

94. Yoshida, H., Nagaoka, A., Kusaka-Kikushima, A., Tobiishi, M., Kawabata, K., Sayo, T., Sakai, S., Sugiyama, Y., Enomoto, H., Okada, Y., and Inoue, S. (2013) KIAA1199, a deafness gene of unknown function, is a new hyaluronan binding protein involved in hyaluronan depolymerization. *Proc Natl Acad Sci U S A*. **110**, 5612–5617

95. Nagaoka, A., Yoshida, H., Nakamura, S., Morikawa, T., Kawabata, K., Kobayashi, M., Sakai, S., Takahashi, Y., Okada, Y., and Inoue, S. (2015) Regulation of Hyaluronan (HA) Metabolism Mediated by HYBID (Hyaluronan-binding Protein Involved in HA Depolymerization, KIAA1199) and HA Synthases in Growth Factor-stimulated Fibroblasts. *J Biol Chem*. **290**, 30910–30923

96. Yamamoto, H., Tobisawa, Y., Inubushi, T., Irie, F., Ohyama, C., and Yamaguchi, Y. (2017) A mammalian homolog of the zebrafish transmembrane protein 2 (TMEM2) is the long-sought-after cell-surface hyaluronidase. *J Biol Chem*. **292**, 7304–7313

97. Simpson, M. A., de la Motte, C., Sherman, L. S., and Weigel, P. H. (2015) Advances in Hyaluronan Biology: Signaling, Regulation, and Disease Mechanisms. *Int J Cell Biol*. 10.1155/2015/690572

98. Pandey, M. S., Baggenstoss, B. A., Washburn, J., Harris, E. N., and Weigel, P. H. (2013) The Hyaluronan Receptor for Endocytosis (HARE) Activates NF-κB-mediated Gene Expression in Response to 40–400-kDa, but Not Smaller or Larger, Hyaluronans. *J. Biol. Chem.* **288**, 14068–14079

99. Collins, S. L., Black, K. E., Chan-Li, Y., Ahn, Y.-H., Cole, P. A., Powell, J. D., and Horton, M. R. (2011) Hyaluronan fragments promote inflammation by down-regulating the anti-inflammatory A2a receptor. *Am J Respir Cell Mol Biol*. **45**, 675–683

100. Scheibner, K. A., Lutz, M. A., Boodoo, S., Fenton, M. J., Powell, J. D., and Horton, M. R. (2006) Hyaluronan Fragments Act as an Endogenous Danger Signal by Engaging TLR2. *The Journal of Immunology*. **177**, 1272–1281

101. Schraufstatter, I., Serobyan, N., DiScipio, R., Feofanova, N., Orlovskaya, I., and Khaldoyanidi, S. K. (2009) Hyaluronan stimulates mobilization of mature hematopoietic cells but not hematopoietic progenitors. *J Stem Cells*. **4**, 191–202

102. Viola, M., Vigetti, D., Karousou, E., D'Angelo, M. L., Caon, I., Moretto, P., De Luca, G., and Passi, A. (2015) Biology and biotechnology of hyaluronan. *Glycoconj J*. **32**, 93–103

103. Ekici, S., Ayhan, A., Kendi, S., and Ozen, H. (2002) Determination of prognosis in patients with prostate cancer treated with radical prostatectomy: prognostic value of CD44v6 score. *J Urol*. **167**, 2037–2041

104. McAtee, C. O., Barycki, J. J., and Simpson, M. A. (2014) Emerging roles for hyaluronidase in cancer metastasis and therapy. *Adv Cancer Res*. **123**, 1–34

105. McAtee, C. O., Booth, C., Elowsky, C., Zhao, L., Payne, J., Fangman, T., Caplan, S., Henry, M. D., and Simpson., M. A. (2019) Prostate tumor cell exosomes containing hyaluronidase Hyal1 stimulate prostate stromal cell motility by engagement of FAK-mediated integrin signaling. *Matrix Biol*. **78–79**, 165–179

106. Simpson, M. A., and Lokeshwar, V. B. (2008) Hyaluronan and hyaluronidase in genitourinary tumors. *Front Biosci*. **13**, 5664–5680

107. Toole, B. P. (2002) Hyaluronan promotes the malignant phenotype. *Glycobiology*. **12**, 37R-42R

108. Fallacara, A., Baldini, E., Manfredini, S., and Vertuani, S. (2018) Hyaluronic Acid in the Third Millennium. *Polymers (Basel)*. 10.3390/polym10070701

109. West, D. C., and Kumar, S. (1989) Hyaluronan and angiogenesis. *Ciba Found Symp*. **143**, 187–201; discussion 201-207, 281–285

110. Pathria, P., Louis, T. L., and Varner, J. A. (2019) Targeting Tumor-Associated Macrophages in Cancer. *Trends Immunol*. **40**, 310–327

111. Josefsson, A., Adamo, H., Hammarsten, P., Granfors, T., Stattin, P., Egevad, L., Laurent, A. E., Wikström, P., and Bergh, A. (2011) Prostate Cancer Increases Hyaluronan in Surrounding Nonmalignant Stroma, and This Response Is Associated with Tumor Growth and an Unfavorable Outcome. *Am J Pathol*. **179**, 1961–1968

112. Pirinen, R., Tammi, R., Tammi, M., Hirvikoski, P., Parkkinen, J. J., Johansson, R., Böhm, J., Hollmén, S., and Kosma, V.-M. (2001) Prognostic value of hyaluronan expression in non-small-cell lung cancer: Increased stromal expression indicates unfavorable outcome in patients with adenocarcinoma. *International Journal of Cancer*. **95**, 12–17

113. Setälä, L. P., Tammi, M. I., Tammi, R. H., Eskelinen, M. J., Lipponen, P. K., Ågren, U. M., Parkkinen, J., Alhava, E. M., and Kosma, V.-M. (1999) Hyaluronan expression in gastric cancer cells is associated with local and nodal spread and reduced survival rate. *British Journal of Cancer*. **79**, 1133–1138

114. Liu, N., Gao, F., Han, Z., Xu, X., Underhill, C. B., and Zhang, L. (2001) Hyaluronan Synthase 3 Overexpression Promotes the Growth of TSU Prostate Cancer Cells. *Cancer Res*. **61**, 5207–5214

115. Kultti, A., Zhao, C., Singha, N. C., Zimmerman, S., Osgood, R. J., Symons, R., Jiang, P., Li, X., Thompson, C. B., Infante, J. R., Jacobetz, M. A., Tuveson, D. A., Frost, G. I., Shepard, H. M., and Huang, Z. (2014) Accumulation of Extracellular Hyaluronan by Hyaluronan Synthase 3 Promotes Tumor Growth and Modulates the Pancreatic Cancer Microenvironment. *BioMed Research International*. **2014**, e817613

116. Bullard, K. M., Kim, H.-R., Wheeler, M. A., Wilson, C. M., Neudauer, C. L., Simpson, M. A., and McCarthy, J. B. (2003) Hyaluronan synthase-3 is upregulated in metastatic colon carcinoma cells and manipulation of expression alters matrix retention and cellular growth. *International Journal of Cancer*. **107**, 739–746

117. Li, Y., Li, L., Brown, T. J., and Heldin, P. (2007) Silencing of hyaluronan synthase 2 suppresses the malignant phenotype of invasive breast cancer cells. *International Journal of Cancer*. **120**, 2557–2567

118. Udabage, L., Brownlee, G. R., Waltham, M., Blick, T., Walker, E. C., Heldin, P., Nilsson, S. K., Thompson, E. W., and Brown, T. J. (2005) Antisense-Mediated Suppression of Hyaluronan Synthase 2 Inhibits the Tumorigenesis and Progression of Breast Cancer. *Cancer Res*. **65**, 6139–6150

119. Twarock, S., Freudenberger, T., Poscher, E., Dai, G., Jannasch, K., Dullin, C., Alves, F., Prenzel, K., Knoefel, W. T., Stoecklein, N. H., Savani, R. C., Homey, B., and Fischer, J. W. (2011) Inhibition of Oesophageal Squamous Cell Carcinoma Progression by in vivo Targeting of Hyaluronan Synthesis. *Mol Cancer*. **10**, 30

120. Okuda, H., Kobayashi, A., Xia, B., Watabe, M., Pai, S. K., Hirota, S., Xing, F., Liu, W., Pandey, P. R., Fukuda, K., Modur, V., Ghosh, A., Wilber, A., and Watabe, K. (2012) Hyaluronan Synthase HAS2 Promotes Tumor Progression in Bone by Stimulating the Interaction of Breast Cancer Stem–Like Cells with Macrophages and Stromal Cells. *Cancer Res*. **72**, 537–547

121. Bharadwaj, A. G., Rector, K., and Simpson, M. A. (2007) Inducible hyaluronan production reveals differential effects on prostate tumor cell growth and tumor angiogenesis. *J Biol Chem*. **282**, 20561–20572

122. Bouga, H., Tsouros, I., Bounias, D., Kyriakopoulou, D., Stavropoulos, M. S., Papageorgakopoulou, N., Theocharis, D. A., and Vynios, D. H. (2010) Involvement of hyaluronidases in colorectal cancer. *BMC Cancer*. **10**, 499

123. Udabage, L., Brownlee, G. R., Nilsson, S. K., and Brown, T. J. (2005) The over-expression of HAS2, Hyal-2 and CD44 is implicated in the invasiveness of breast cancer. *Experimental Cell Research*. **310**, 205–217

124. Chi, A., Shirodkar, S. P., Escudero, D. O., Ekwenna, O. O., Yates, T. J., Ayyathurai, R., Garcia-Roig, M., Gahan, J. C., Manoharan, M., Bird, V. G., and Lokeshwar, V. B. (2012) Molecular characterization of kidney cancer. *Cancer*. **118**, 2394–2402

125. Li, Y., Wang, D., Wang, L., Yu, J., Du, D., Chen, Y., Gao, P., Wang, D.-M., Yu, J., Zhang, F., and Fu, S. (2013) Distinct Genomic Aberrations between Low-Grade and High-Grade Gliomas of Chinese Patients. *PLoS One*. **8**, e57168

126. Beech, D. J., Madan, A. K., and Deng, N. (2002) Expression of PH-20 in Normal and Neoplastic Breast Tissue. *Journal of Surgical Research*. **103**, 203–207

127. Madan, A. K., Pang, Y., Wilkiemeyer, M. B., Yu, D., and Beech, D. J. (1999) Increased hyaluronidase expression in more aggressive prostate adenocarcinoma. *Oncol Rep.* **6**, 1431–1433

128. Eissa, S., Swellam, M., Shehata, H., El-Khouly, I. M., El-Zayat, T., and El-Ahmady, O. (2010) Expression of HYAL1 and Survivin RNA as Diagnostic Molecular Markers for Bladder Cancer. *The Journal of Urology*. **183**, 493–498

129. Eissa, S., Zohny, S. F., Shehata, H. H., Hegazy, M. G. A., Salem, A. M., and Esmat, M. (2012) Urinary retinoic acid receptor-β2 gene promoter methylation and hyaluronidase activity as noninvasive tests for diagnosis of bladder cancer. *Clinical Biochemistry*. **45**, 402–407

130. Tan, J.-X., Wang, X.-Y., Li, H.-Y., Su, X.-L., Wang, L., Ran, L., Zheng, K., and Ren, G.-S. (2011) HYAL1 overexpression is correlated with the malignant behavior of human breast cancer. *International Journal of Cancer*. **128**, 1303–1315

131. Kramer, M. W., Escudero, D. O., Lokeshwar, S. D., Golshani, R., Ekwenna, O. O., Acosta, K., Merseburger, A. S., Soloway, M., and Lokeshwar, V. B. (2011) Association of hyaluronic acid family members (HAS1, HAS2, and HYAL-1) with bladder cancer diagnosis and prognosis. *Cancer*. **117**, 1197–1209

132. Yoffou, P. H., Edjekouane, L., Meunier, L., Tremblay, A., Provencher, D. M., Mes-Masson, A.-M., and Carmona, E. (2011) Subtype specific elevated expression of hyaluronidase-1 (HYAL-1) in epithelial ovarian cancer. *PLoS One*. **6**, e20705

133. Cheng, X.-B., Sato, N., Kohi, S., and Yamaguchi, K. (2013) Prognostic Impact of Hyaluronan and Its Regulators in Pancreatic Ductal Adenocarcinoma. *PLoS One*. 10.1371/journal.pone.0080765

134. de Sá, V. K., Olivieri, E., Parra, E. R., Ab'Saber, A. M., Takagaki, T., Soares, F. A., Carraro, D., Carvalho, L., and Capelozzi, V. L. (2012) Hyaluronidase splice variants are associated with histology and outcome in adenocarcinoma and squamous cell carcinoma of the lung. *Human Pathology*. **43**, 675–83

135. Bharadwaj, A. G., Goodrich, N. P., McAtee, C. O., Haferbier, K., Oakley, G. G., Wahl, J. K., and Simpson, M. A. (2011) Hyaluronan suppresses prostate tumor cell proliferation through diminished expression of N-cadherin and aberrant growth factor receptor signaling. *Exp Cell Res*. **317**, 1214–1225

136. Kovar, J. L., Johnson, M. A., Volcheck, W. M., Chen, J., and Simpson, M. A. (2006) Hyaluronidase Expression Induces Prostate Tumor Metastasis in an Orthotopic Mouse Model. *Am J Pathol*. **169**, 1415–1426

137. Lokeshwar, V. B., Cerwinka, W. H., and Lokeshwar, B. L. (2005) HYAL1 Hyaluronidase: A Molecular Determinant of Bladder Tumor Growth and Invasion. *Cancer Res*. **65**, 2243–2250

138. Shuster, S., Frost, G. I., Csoka, A. B., Formby, B., and Stern, R. (2002) Hyaluronidase reduces human breast cancer xenografts in SCID mice. *Int J Cancer*. **102**, 192–197

139. Lokeshwar, V. B., Cerwinka, W. H., Isoyama, T., and Lokeshwar, B. L. (2005) HYAL1 hyaluronidase in prostate cancer: a tumor promoter and suppressor. *Cancer Res.* **65**, 7782–7789

140. Chanmee, T., Ontong, P., Izumikawa, T., Higashide, M., Mochizuki, N., Chokchaitaweesuk, C., Khansai, M., Nakajima, K., Kakizaki, I., Kongtawelert, P., Taniguchi, N., and Itano, N. (2016) Hyaluronan Production Regulates Metabolic and Cancer Stem-like Properties of Breast Cancer Cells via Hexosamine Biosynthetic Pathway-coupled HIF-1 Signaling. *J Biol Chem.* **291**, 24105–24120

141. Terabe, K., Ohashi, Y., Tsuchiya, S., Ishizuka, S., Knudson, C. B., and Knudson, W. (2019) Chondroprotective effects of 4-methylumbelliferone and hyaluronan synthase-2 overexpression involve changes in chondrocyte energy metabolism. *J Biol Chem.* **294**, 17799–17817

142. Honda, T., Kaneiwa, T., Mizumoto, S., Sugahara, K., and Yamada, S. (2012) Hyaluronidases Have Strong Hydrolytic Activity toward Chondroitin 4-Sulfate Comparable to that for Hyaluronan. *Biomolecules.* **2**, 549–563

143. Gushulak, L., Hemming, R., Martin, D., Seyrantepe, V., Pshezhetsky, A., and Triggs-Raine, B. (2012) Hyaluronidase 1 and β-Hexosaminidase Have Redundant Functions in Hyaluronan and Chondroitin Sulfate Degradation♦. *J Biol Chem.* **287**, 16689–16697

144. Csoka, A. B., Frost, G. I., and Stern, R. (2001) The six hyaluronidase-like genes in the human and mouse genomes. *Matrix Biol.* **20**, 499–508

145. Lv, S.-H., Rong, S.-F., Cai, B.-G., Guan, S.-M., and Li, Q.-Q. (2015) Property and current clinical applications of mammal hyaluronidase. *Eur Rev Med Pharmacol Sci*. **19**, 3968–3976

146. Puissant, E., Gilis, F., Dogné, S., Flamion, B., Jadot, M., and Boonen, M. (2014) Subcellular trafficking and activity of Hyal-1 and its processed forms in murine macrophages. *Traffic*. **15**, 500–515

147. Lepperdinger, G., Strobl, B., and Kreil, G. (1998) HYAL2, a human gene expressed in many cells, encodes a lysosomal hyaluronidase with a novel type of specificity. *J Biol Chem*. **273**, 22466–22470

148. Lepperdinger, G., Müllegger, J., and Kreil, G. (2001) Hyal2--less active, but more versatile? *Matrix Biol*. **20**, 509–514

149. Harada, H., and Takahashi, M. (2007) CD44-dependent Intracellular and Extracellular Catabolism of Hyaluronic Acid by Hyaluronidase-1 and -2. *J. Biol. Chem.* **282**, 5597–5607

150. Atmuri, V., Martin, D. C., Hemming, R., Gutsol, A., Byers, S., Sahebjam, S., Thliveris, J. A., Mort, J. S., Carmona, E., Anderson, J. E., Dakshinamurti, S., and Triggs-Raine, B. (2008) Hyaluronidase 3 (HYAL3) knockout mice do not display evidence of hyaluronan accumulation. *Matrix Biol*. **27**, 653–660

151. Hemming, R., Martin, D. C., Slominski, E., Nagy, J. I., Halayko, A. J., Pind, S., and Triggs-Raine, B. (2008) Mouse Hyal3 encodes a 45- to 56-kDa glycoprotein whose overexpression increases hyaluronidase 1 activity in cultured cells. *Glycobiology*. **18**, 280–289

152. Kaneiwa, T., Mizumoto, S., Sugahara, K., and Yamada, S. (2010) Identification of human hyaluronidase-4 as a novel chondroitin sulfate hydrolase that preferentially cleaves the galactosaminidic linkage in the trisulfated tetrasaccharide sequence. *Glycobiology*. **20**, 300–309

153. Cherr, G. N., Meyers, S. A., Yudin, A. I., VandeVoort, C. A., Myles, D. G., Primakoff, P., and Overstreet, J. W. (1996) The PH-20 protein in cynomolgus macaque spermatozoa: identification of two different forms exhibiting hyaluronidase activity. *Dev Biol.* **175**, 142–153

154. Arming, S., Strobl, B., Wechselberger, C., and Kreil, G. (1997) In vitro mutagenesis of PH-20 hyaluronidase from human sperm. *European journal of biochemistry*. **247**, 810–814

155. Elson, L. A., and Morgan, W. T. J. (1933) A colorimetric method for the determination of glucosamine and chondrosamine. *Biochemical Journal*. **27**, 1824–1828

156. Reissig, J. L., Strominger, J. L., and Leloir, L. F. (1955) A MODIFIED COLORIMETRIC METHOD FOR THE ESTIMATION OF N-ACETYLAMINO SUGARS. *Journal of Biological Chemistry*. **217**, 959–966

157. Takahashi, T., Ikegami-Kawai, M., Okuda, R., and Suzuki, K. (2003) A fluorimetric Morgan–Elson assay method for hyaluronidase activity. *Analytical Biochemistry*. **322**, 257–263

158. Wingfield, P. T. (2001) Protein Precipitation Using Ammonium Sulfate. *Curr Protoc Protein Sci*. **APPENDIX 3**, Appendix-3F

159. Lenormand, H., Deschrevel, B., and Vincent, J.-C. (2010) pH effects on the hyaluronan hydrolysis catalysed by hyaluronidase in the presence of proteins: Part I. Dual aspect of the pH-dependence. *Matrix Biology*. **29**, 330–337

160. Guillemette, C. (2003) Pharmacogenomics of human UDP-glucuronosyltransferase enzymes. *Pharmacogenomics J.* **3**, 136–158

161. Ritter, J. K. (2000) Roles of glucuronidation and UDP-glucuronosyltransferases in xenobiotic bioactivation reactions. *Chem Biol Interact*. **129**, 171–193

162. Tukey, R. H., and Strassburg, C. P. (2000) Human UDP-glucuronosyltransferases: metabolism, expression, and disease. *Annu Rev Pharmacol Toxicol*. **40**, 581–616

163. Cummings, J., Boyd, G., Ethell, B. T., Macpherson, J. S., Burchell, B., Smyth, J. F., and Jodrell, D. I. (2002) Enhanced clearance of topoisomerase I inhibitors from human colon cancer cells by glucuronidation. *Biochem Pharmacol*. **63**, 607–613

164. Cummings, J., Ethell, B. T., Jardine, L., Boyd, G., Macpherson, J. S., Burchell, B., Smyth, J. F., and Jodrell, D. I. (2003) Glucuronidation as a mechanism of intrinsic drug resistance in human colon cancer: reversal of resistance by food additives. *Cancer Res*. **63**, 8443–8450

165. de Almagro, M. C., Selga, E., Thibaut, R., Porte, C., Noé, V., and Ciudad, C. J. (2011) UDP-glucuronosyltransferase 1A6 overexpression in breast cancer cells resistant to methotrexate. *Biochem Pharmacol*. **81**, 60–70

166. Oguri, T., Takahashi, T., Miyazaki, M., Isobe, T., Kohno, N., Mackenzie, P. I., and Fujiwara, Y. (2004) UGT1A10 is responsible for SN-38 glucuronidation and its expression in human lung cancers. *Anticancer Res*. **24**, 2893–2896

167. Heldin, P., Basu, K., Kozlova, I., and Porsch, H. (2014) Chapter Eight - HAS2 and CD44 in Breast Tumorigenesis. in *Advances in Cancer Research* (Simpson, M. A., and Heldin, P. eds), pp. 211–229, Hyaluronan Signaling and Turnover, Academic Press, **123**, 211–229

168. Stamenkovic, I., Aruffo, A., Amiot, M., and Seed, B. (1991) The hematopoietic and epithelial forms of CD44 are distinct polypeptides with different adhesion potentials for hyaluronate-bearing cells. *EMBO J*. **10**, 343–348

169. Stamenkovic, I., Amiot, M., Pesando, J. M., and Seed, B. (1989) A lymphocyte molecule implicated in lymph node homing is a member of the cartilage link protein family. *Cell*. **56**, 1057–1062

170. Günthert, U., Hofmann, M., Rudy, W., Reber, S., Zöller, M., Haussmann, I., Matzku, S., Wenzel, A., Ponta, H., and Herrlich, P. (1991) A new variant of glycoprotein CD44 confers metastatic potential to rat carcinoma cells. *Cell*. **65**, 13–24

171. Wu, C.-H., Liu, I.-J., Lu, R.-M., and Wu, H.-C. (2016) Advancement and applications of peptide phage display technology in biomedical science. *Journal of Biomedical Science*. **23**, 8

172. Mund, T., Lewis, M. J., Maslen, S., and Pelham, H. R. (2014) Peptide and small molecule inhibitors of HECT-type ubiquitin ligases. *Proc Natl Acad Sci U S A*. **111**, 16736–16741

173. Lin, S.-H., Chang, D.-K., Chou, M.-J., Huang, K.-J., and Shiuan, D. (2015) Peptide inhibitors of human HMG-CoA reductase as potential hypocholesterolemia agents. *Biochemical and Biophysical Research Communications*. **456**, 104–109

174. Lee, Y.-C., Hsiao, N.-W., Tseng, T.-S., Chen, W.-C., Lin, H.-H., Leu, S.-J., Yang, E.-W., and Tsai, K.-C. (2015) Phage display-mediated discovery of novel tyrosinase-targeting tetrapeptide inhibitors reveals the significance of N-terminal preference of cysteine residues and their functional sulfur atom. *Mol Pharmacol*. **87**, 218–230

175. Kofler, M., Motzny, K., Beyermann, M., and Freund, C. (2005) Novel interaction partners of the CD2BP2-GYF domain. *J Biol Chem*. **280**, 33397–33402

176. Kärkkäinen, S., Hiipakka, M., Wang, J.-H., Kleino, I., Vähä-Jaakkola, M., Renkema, G. H., Liss, M., Wagner, R., and Saksela, K. (2006) Identification of preferred protein

interactions by phage-display of the human Src homology-3 proteome. *EMBO Rep*. **7**, 186–191

177. Abu-Odeh, M., Bar-Mag, T., Huang, H., Kim, T., Salah, Z., Abdeen, S. K., Sudol, M., Reichmann, D., Sidhu, S., Kim, P. M., and Aqeilan, R. I. (2014) Characterizing WW domain interactions of tumor suppressor WWOX reveals its association with multiprotein networks. *J Biol Chem*. **289**, 8865–8880

178. Deng, S.-J., Pearce, K. H., Dixon, E. P., Hartley, K. A., Stanley, T. B., Lobe, D. C., Garvey, E. P., Kost, T. A., Petty, R. L., Rocque, W. J., Alexander, K. A., and Underwood, M. R. (2004) Identification of peptides that inhibit the DNA binding, trans-activator, and DNA replication functions of the human papillomavirus type 11 E2 protein. *J Virol*. **78**, 2637–2641

179. Kim, H., and Ho, M. (2018) Current Protocols in Protein Science. *Curr Protoc Protein Sci*. **94**, e66

180. Otwinowski, Z., and Minor, W. (1997) Processing of X-ray diffraction data collected in oscillation mode. *Methods in Enzymology*. **276**, 307–326

181. Adams, P. D., Afonine, P. V., Bunkóczi, G., Chen, V. B., Davis, I. W., Echols, N., Headd, J. J., Hung, L.-W., Kapral, G. J., Grosse-Kunstleve, R. W., McCoy, A. J., Moriarty, N. W., Oeffner, R., Read, R. J., Richardson, D. C., Richardson, J. S., Terwilliger, T. C., and Zwart, P. H. (2010) PHENIX: a comprehensive Python-based system for macromolecular structure solution. *Acta Crystallogr D Biol Crystallogr*. **66**, 213–221

182. Emsley, P., Lohkamp, B., Scott, W. G., and Cowtan, K. (2010) Features and development of Coot. *Acta Crystallogr D Biol Crystallogr*. **66**, 486–501

183. Karplus, P. A., and Diederichs, K. (2012) Linking crystallographic model and data quality. *Science*. **336**, 1030–1033

184. Diederichs, K., and Karplus, P. A. (1997) Improved R-factors for diffraction data analysis in macromolecular crystallography. *Nat Struct Biol*. **4**, 269–275

185. Yesudasu, V., Pradhan, H. S., and Pandya, R. J. (2021) Recent progress in surface plasmon resonance based sensors: A comprehensive review. *Heliyon.* **7**, e06321

186. Hilt, S., Rojalin, T., Viitala, T., Koivuniemi, A., Bunker, A., Wachsmann-Hogiu, S., Kálai, T., Hideg, K., Yliperttula, M., and Voss, J. C. (2017) Oligomerization Alters Binding Affinity between Amyloid Beta and a Modulator of Peptide Aggregation. *J. Phys. Chem. C*. **121**, 23974–23987

187. Juhász, Á., Csapó, E., Ungor, D., Tóth, G. K., Vécsei, L., and Dékány, I. (2016) Kinetic and Thermodynamic Evaluation of Kynurenic Acid Binding to GluR1270–300 Polypeptide by Surface Plasmon Resonance Experiments. *J. Phys. Chem. B*. **120**, 7844–7850

188. Wang, Y., Wang, G., Moitessier, N., and Mittermaier, A. K. (2020) Enzyme Kinetics by Isothermal Titration Calorimetry: Allostery, Inhibition, and Dynamics. *Front. Mol. Biosci.* 10.3389/fmolb.2020.583826